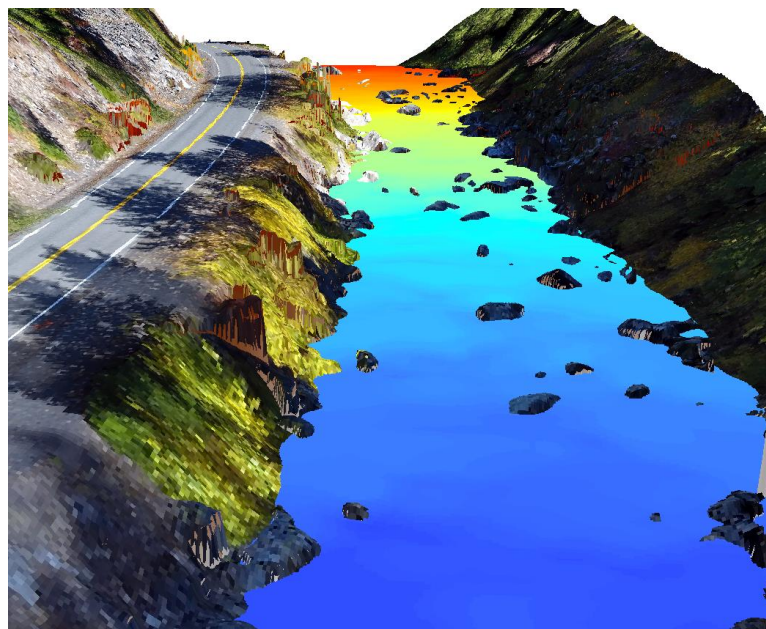


SOUTH FORK CLEARWATER RIVER

MP 28 Hypothesized Velocity Barrier

Final Report



Prepared for:

Mark Johnson, Nez Perce Tribe

Prepared by:

Ray Timm, Lucius Caldwell, Dana Stroud, and Phil Roni – Cramer Fish Sciences

Andrew Nelson, Chris Long – Northwest Hydraulic Consultants

January 18, 2017

EXECUTIVE SUMMARY

In summer 2016, Nez Perce Tribe (NPT) contracted with Cramer Fish Sciences (CFS) for assistance surveying, modeling, and analyzing a reach of the South Fork (SF) Clearwater River (Idaho), to determine if one or more velocity barriers exist during spring flows that prevent adult steelhead (*Oncorhynchus mykiss*) migration to upstream spawning habitat. NPT staff hypothesized that a barrier emerges within this reach at discharges above approximately 600 cfs at the USGS gage upstream near Elk City, limiting successful steelhead migration.

Data from a series of unmanned aerial vehicle flights and a traditional thalweg survey were used to develop a model of channel geometry within the study reach. From this physical model, a series of hydraulic model iterations were then run at increasing discharge, in order to estimate velocity within 2 ft grid cells that covered the entire stream channel. Next, fish burst swimming speeds were overlaid on these grid cell velocity estimates to assess whether a 90 cm steelhead (similar in size to a large three ocean year Clearwater B-run fish) could pass, based on published critical swimming velocities (V_{crit}). Thus, grid cell velocity and length of patches with similar velocity were both taken into account to determine passability. Next, a series of climate model flow scenarios were used to infer the likelihood of a change in the frequency of occurrence of such a barrier. Finally, adult steelhead tracking data were used to test fish passage of the hypothesized barrier in relation to discharge and to fish fork length at the time of tagging. In this way, available data were used to evaluate the hypothesis that velocities within the study reach prevent all but the largest fish from passing, and thus constitute an environmental selection filter that contributes to “B-run” qualities.

Hydraulic modeling efforts revealed that high velocity patches, that require steelhead to swim at burst speeds sustainable for less than 20 seconds, appear at discharge within the study reach as low as 100 cfs. These are likely passage impediments, which prevent fish with low energy reserves or low aerobic capacity from passing. Increasing discharge was associated with an increasing frequency and spatial extent of these passage impediments. Moreover, above approximately 1,000 cfs, velocity at a single patch within the study reach exceed V_{crit} for a 90 cm steelhead. At higher discharge, up to 4 patches within the study reach exhibited velocities that exceed V_{crit} for a 90 cm steelhead, and more than 450 patches could constitute additional barriers to upstream adult steelhead passage by virtue of their combined velocity and length. Thus, the modeling efforts support NPT’s observations and *a priori* hypothesis that a velocity barrier within the reach exists at discharge similar to that encountered annually during spring freshet.

Climate model flow scenarios suggest a change in both magnitude and timing of spring freshet to an earlier, smaller spring seasonal flood. However, models also suggest an increase in the magnitude of large floods (20 to 100 year recurrence interval). These shifts may lead to a reduction in the intensity of the spring freshet associated barrier, but an increase in recurrence of barrier emergence during other times of the year. It is difficult to predict how the barrier will respond to this forecast shift. But, it seems possible that, given the low discharge threshold necessary for the barrier to set up, under these scenarios the barrier will likely persist, and may emerge both earlier during steelhead spawning migration and potentially at other times of the year as well.

South Fork Clearwater River MP 28 Hypothesized Velocity Barrier

Tracking data provided by the NPT were evaluated in order to empirically test passage of the hypothesized barrier. Thirteen radio tagged steelhead successfully passed the hypothesized barrier during periods when mean discharge at Elk City was 742 – 837 cfs. Two fish successfully passed the hypothesized barrier during a period when discharge at Elk City was as high as 1,380 cfs, although the precise date of their passage cannot be inferred from the available data. If analysis is restricted to the more highly reliable subset of seven of these 13 fish (omitting fish with only one detection and omitting the two aforementioned outlier fish whose precise date of passage cannot be inferred), then steelhead can be inferred to have successfully passed the hypothesized barrier when discharge at Elk City was 670 – 692 cfs.

In conclusion, a velocity barrier preventing upstream migration of adult steelhead appears to emerge within the study reach. At discharge as low as 100 cfs, certain areas of this reach of the SF Clearwater may be impassable, even for a 90 cm steelhead. However, these low discharge velocities should be more appropriately thought of as impediments. Although published literature indicates that steelhead can sustain a particular swimming pace only for a defined duration, it may be the case that particularly “fit” steelhead may be able to swim slightly faster for slightly longer. (Moreover, such remarkably high aerobic scope or otherwise elevated performance may partially underlie “B-run” character.) Once discharge reaches approximately 1,000 cfs within the reach, however, at least one velocity barrier emerges, which would appear to exhaust the theoretical upper limit of swimming velocity capacity for a 90 cm steelhead. As discharge increases further, the number of both impediments and barriers increases, as does the likelihood that these features operationally restrict upstream steelhead migration. Nonetheless, empirical tracking data suggest that some fish may pass the barrier when discharge is sufficient to create an apparent barrier. Resolving this discrepancy may involve 1) further testing swimming capacity of SF Clearwater B-run steelhead or 2) designing a more rigorous experiment (e.g., a telemetry study focusing on evaluating passage through the hypothesized barrier) to evaluate fish passage within the study reach.

It may be possible to mitigate some, though not all, of the barriers and impediments present in this high velocity reach. However, we suggest that an additional, focused telemetry study be conducted first. Determining whether mitigation *could* and *should* be considered further would be enabled with a rigorous empirical study to resolve the passage performance of regional steelhead. In addition, mitigation scenario modeling could help ensure efficacy of actions ultimately taken.

Acknowledgement of Funding Agency:

Radio Tags, the South Fork Clearwater tagging effort, and the radio telemetry data collection were funded by Bonneville Power Administration Project #2010-057-00, B-run Steelhead Supplementation Effectiveness Research. Funding for the investigation into the barrier by NPT and by Cramer are funded by Bonneville Power Administration Project #2010-003-00, Lower South Fork Clearwater/Slate Creek Watershed Restoration and by funding made available by the Snake River Basin Adjudication (SRBA).

TABLE OF CONTENTS

Executive Summary	i
Acknowledgement of Funding Agency:	ii
Table of Contents	iii
List of Figures	iv
List of Tables	iv
Introduction	5
Purpose and Need	5
Study Area: South Fork Clearwater River	5
Approach	6
Methods	7
Geomorphic, Fish Habitat, and Fish Passage Barrier Survey	7
Field Survey	7
Data Processing and Surface Development	10
Hydraulic and Hydrologic Analyses	12
Fish Contextualization	25
Modeling Fish Burst Swimming Performance	27
Fish Behaviors Inferred from Tracking Data	27
Results	29
Geomorphic, Fish Habitat, and Fish Passage Barrier Survey	29
Field Survey & Surface Development	29
Hydraulic and Hydrologic Analyses	32
Fish Contextualization	40
Modeling Fish Burst Swimming Performance	40
Fish Behaviors Inferred from Tracking Data	41
Discussion	46
Is there a barrier? – Does channel morphology near MP 28 interact with regional hydrology to create sufficient velocities that steelhead passage is likely impeded or prevented?	46
Hydraulic Model Inference	46
Tracking Data Inference	49
Do we expect this barrier prevents all fish from passing, or could there be a size threshold? ..	50
How frequently, and at what times during the year, does a barrier emerge?	50
Are these also times when we anticipate fish being present in the study area?	50
Will the barrier appear more frequently or less frequently in the future?	51
What do we know about the cause of the barrier?	51
What can potentially be done about the barrier?	51
What additional studies may be required?	52
References	53
Appendix A: Pix4D Quality Control Report	55
Appendix B: Complete Orthophoto Mosaic	56
Appendix C: Complete Merged Surface	57
Appendix D: Frequency of Velocity Barriers at Increasing Discharge	58

List of Figures

Figure 1. Orthogonalized aerial photos of the project area.....	6
Figure 2. Location map (top), discharge (middle), and observed stage (bottom) at Elk City	8
Figure 3. Examples of channel morphologies.....	10
Figure 4. Study reach segmented by drone survey zones.	10
Figure 5. Locations of USGS gages and boundaries for contributing watersheds	12
Figure 6. Scaled flow exceedance curve evaluated for the project site.	13
Figure 7. Complete DEM with hydraulic model domain highlighted.	15
Figure 8. Computed water depth vs. computation time at three locations.....	16
Figure 9. 2-foot grid overlying scaled image of typical streambed in study reach.....	17
Figure 10. Computed water surface elevation (top) and velocity (bottom)	19
Figure 11. Orthophoto, modeled flow depth, and velocity	21
Figure 12. Frequency of occurrence of difference between measured and computed depth.....	22
Figure 13. Comparison of photo (top) and model results (bottom)	23
Figure 14. Modeled velocity and water surface elevation	24
Figure 15. Diagram coupling upstream burst speed capability with downstream flow.....	26
Figure 16. Surveyed thalweg and water surface profiles	30
Figure 17. Example of orthophoto mosaic (left) and digital elevation model (right)	31
Figure 18. Peak flows and fitted distributions for the SF Clearwater River near Elk City.....	32
Figure 19. Peak flows and fitted distributions for the SF Clearwater River near Grangeville. ...	33
Figure 20. Ratio of computed flow in project reach (Q_{PR}) to flow at Elk City (Q_{EC}).....	34
Figure 21. Raster hydrograph showing daily flows for period of record.....	35
Figure 22. Annual hydrograph at project site with daily percent exceedance curves.....	36
Figure 23. Summary of projected monthly flow (given in inches) changes	37
Figure 24. Summary of predicted flood flow changes for several of the analog locations	38
Figure 25. Emergence of barriers within the study reach	40
Figure 26. Extents of hydraulic barriers in one area of concern	41
Figure 27. Temporal distribution showing detections in study area	42
Figure 28. Relative proportion of tagged steelhead that successfully passed.....	42
Figure 29. Daily counts of fish detected	43
Figure 30. Comparison of fork length (FL) among Failed, Passed, and Did Not Enter	45
Figure 31. Fish #128's RT detection history.....	46
Figure 32. Example of chaotic patterns	49

List of Tables

Table 1. Summary of basin characteristics for project area	14
Table 2. Final Model Parametrization.....	20
Table 3. Calculated flood discharges	34
Table 4. RT detections of successfully passing fish.....	44
Table 5. Emergence of discrete patches that impede upstream swimming.....	58

INTRODUCTION

Purpose and Need

Concerns about potential hydraulic barriers to steelhead (*Oncorhynchus mykiss*) migration near river mile 44 (RKM 71) in the South Fork (SF) Clearwater River prompted this investigation. Two independent lines of evidence demonstrate that a velocity barrier emerges under spring discharge regimes, impeding upstream adult steelhead spawning migration. First, adult Chinook salmon successfully migrate through the reach under fall discharges and spawn successfully upstream. Second, radio-tagged adult steelhead are observed entering the reach of concern at greater frequency than with which they successfully pass the upstream extent of the reach. Data from radio tagged adult steelhead indicate that conditions in the study reach create an upstream migration barrier under flows that coincide with migration timing (see *Fish Behaviors Inferred from Tracking Data*, below). This is problematic because of the extent of high quality spawning habitat that exists above the study reach.

The focus of the current study was to provide a detailed hydraulic analysis of the magnitude and spatial extent of potential hydraulic barriers in a study reach of the SF Clearwater River near Golden, Idaho. Hydraulic modeling output was then used as the starting point for a series of calculations to assess the ability of steelhead to migrate through the study reach. In addition, steelhead tracking data provided by Nez Perce Tribe (NPT) were used to empirically assess and validate model output, in order to test hypotheses regarding passage and discharge.

Owing to the cultural and ecological significance of steelhead (see CRITFC 2014), and the proportion of valuable spawning and rearing habitat that exists upstream of the suspected barrier reach, this effort centered on identifying the magnitude of discharge at which hydraulic conditions develop in the channel that prevent steelhead from reaching their upstream spawning grounds. The resulting 2-D hydraulic model outputs provide a path forward for addressing specific locations in the channel where these hydraulic barriers are most likely to establish, which can be used to inform potential mitigation options if those are considered in the future by NPT. The range of flows under which these situations develop are examined, as well as their frequency. Also, we present discussion related to future climate modeling that has implications for fish passage under expected future changing precipitation regimes.

Study Area: South Fork Clearwater River

To reach the project area (Figure 1) on their migration to the SF Clearwater River from the North Pacific Ocean, steelhead traverse nearly 1,000 river kilometers and eight mainstem dams. Historic steelhead escapement above what is now Lower Granite Dam approached 115,000 fish on an annual basis (USFWS 2012). More recent estimates by the Idaho Department of Fish and Game (IDFG) for the years of 1994-2003 indicate total steelhead escapement to the Snake River ranging from 273 to 6,895 with a mean of approximately 2,000 fish per year (USFWS 2012). Current mandates require at least 14,000 adult steelhead to reach the area upstream of the Lower Granite Dam (USFWS 2012), meaning that escapement is well below the target of resource management agencies.

South Fork Clearwater River MP 28 Hypothesized Velocity Barrier

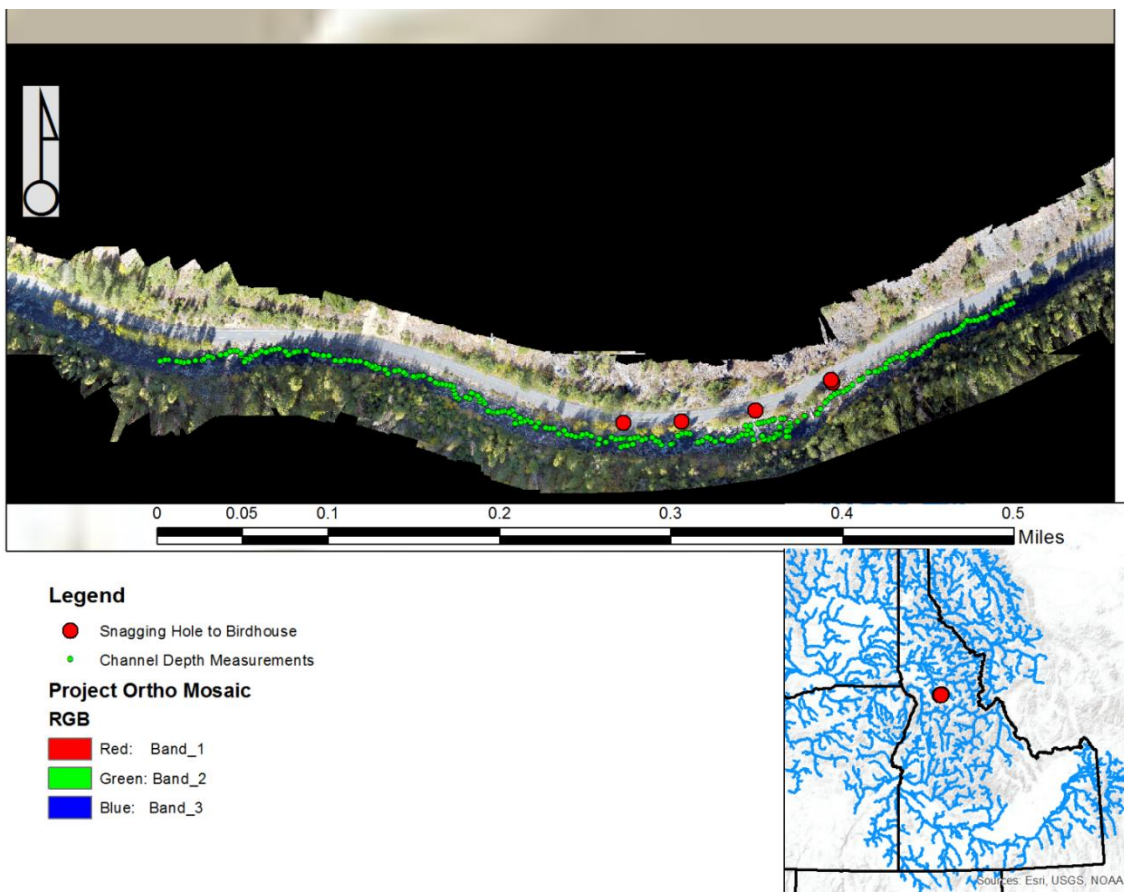


Figure 1. Orthogonalized aerial photos of the project area on the SF Clearwater River. Green dots represent channel bed surface elevation measurements. Red dots represent the study target area from “birdhouse” to “snagging hole.”

Approach

To assess the likelihood that the conditions present at the purported RKM 71 velocity barrier prevent upstream migration of adult steelhead, we adopted the following approach:

- Survey the study site with a combination of aerial photography and thalweg profile
- Use survey data to develop a georeferenced model of channel geometry
- Use modeled channel geometry to develop model of in-stream hydraulics across relevant discharges
- Assess whether in-stream hydraulics create sufficient velocities to prevent adult steelhead from swimming upstream. If so, determine the following:
 - Discharge at which barriers emerge, and
 - Expected frequency of such barriers under current and projected future conditions
- Analyze NPT adult steelhead tracking data to evaluate fish passage through the study site, and test/validate hydraulic model output

METHODS

Geomorphic, Fish Habitat, and Fish Passage Barrier Survey

Field Survey

Overview of approach

Field survey activities were performed by a collaborative team of CFS and NHC staff, including a fish biologist, fluvial geomorphologist, and hydraulic engineer. In addition to general observations of hydraulic conditions and reach-scale geomorphology, three principal classes of topographic information were collected to construct a topographic surface of the project reach:

- 1) Ground- and survey control points were set utilizing real time kinematic (RTK) global positioning system (GPS) data,
- 2) A profile through the channel thalweg was surveyed using a total station, and
- 3) Nadir (downward facing) photos were collected using a lightweight small unmanned aircraft system (sUAS).

The sUAS photos were subsequently processed using structure from motion (SFM) techniques (Fonstad et al. 2013; Javernick et al. 2014; Westoby et al. 2012) to produce an extremely detailed orthophoto mosaic and digital surface model (DSM) of the project area. These data were merged with LiDAR and the thalweg profile survey to produce a Digital Elevation Model (DEM) representing the channel topography for use in hydraulic modeling.

Field survey of the channel occurred between September 25th and 26th, 2016, during the declining limb of the second autumn flow pulse and following a small precipitation event. Flows at the nearest upstream gage (USGS 13337500 “SF Clearwater River near Elk City”; Figure 2, top panel) had peaked at approximately 130 cfs on September 22nd, then slowly declined to approximately 48 cfs at the beginning of survey work on September 25th, and further declined to 38 cfs by the completion of work on September 26th (Figure 2, middle panel). Corresponding stage at the gage site varied by approximately 2 inches (5 cm; Figure 2, bottom panel).

GPS Control point surveys

The control survey was conducted utilizing two Magellan Promark 500 RTK GPS rovers and a Trimble R10 RTK GPS configured as a base station. A local horizontal survey datum was used because no preexisting high-quality horizontal survey control was available near the project site. Comparison of surveyed control points against landmarks visible in existing orthophotos suggest the horizontal accuracy of the local survey datum was within the resolution of the best available aerial photos for comparison. In contrast, vertical elevations were tied to a first order vertical survey control (National Geodetic Survey point QZ0508), which was located just downstream of the project area. This control point had been established via a level loop and provided precise vertical control, but its horizontal position had been determined only by location on a topographic map. Therefore, the horizontal control had less accuracy than could be determined with DGPS and was not considered further, leading us to set our own horizontal control point.

 South Fork Clearwater River MP 28 Hypothesized Velocity Barrier

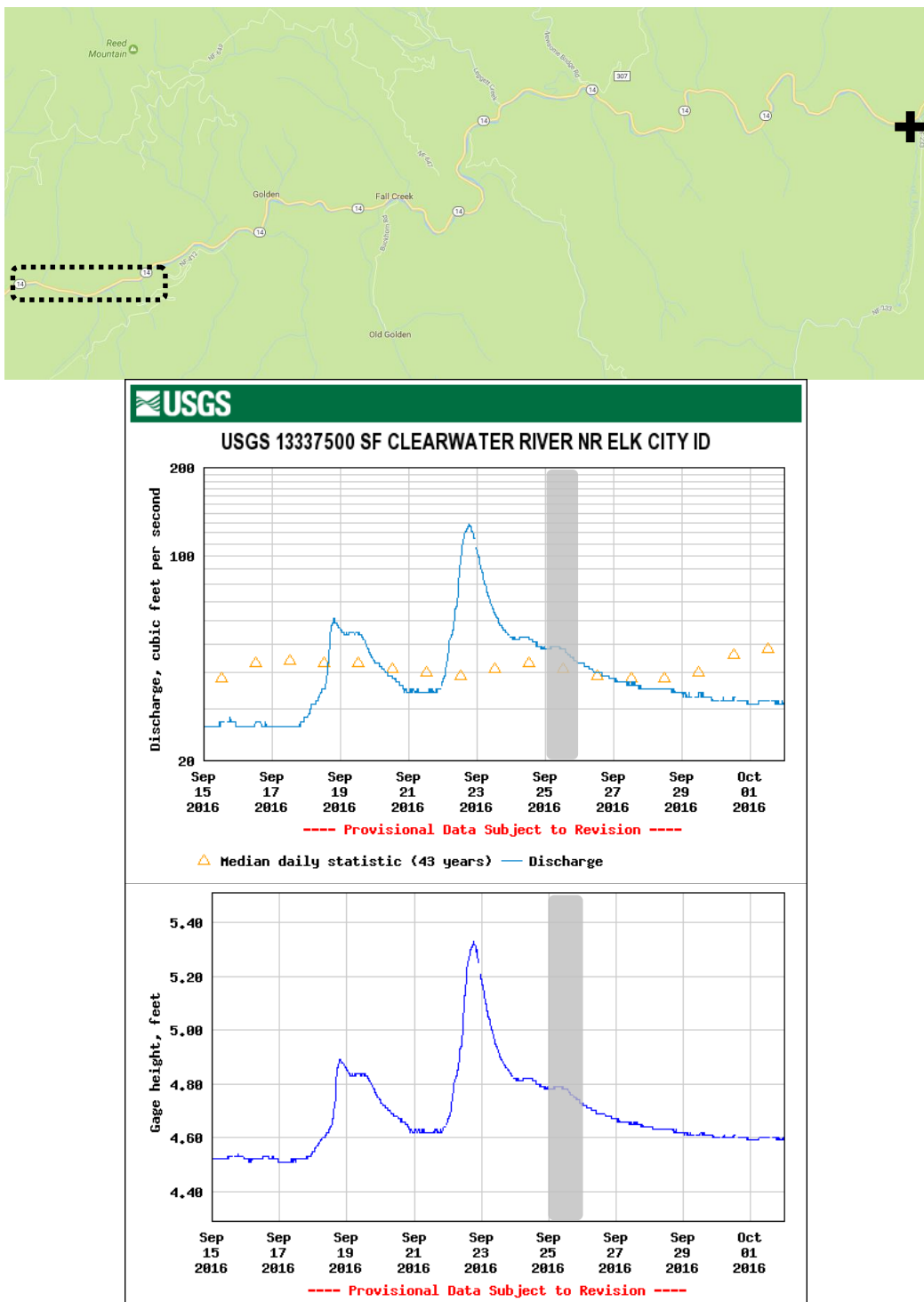


Figure 2. Location map (top), showing approximate location of USGS gage 13337500 (“SF Clearwater River Near Elk City ID,” indicated by solid black cross), relative to approximate project study reach location (enclosed by dotted black rectangle). Discharge (middle) and observed stage (bottom) at the USGS Elk City gage during late September / early October 2016. Map courtesy of Google Maps. Data and plots courtesy of USGS (2016a). Shaded gray rectangles in middle and bottom panels denote sampling period.

South Fork Clearwater River MP 28 Hypothesized Velocity Barrier

Range limitations for the radio required setting up the base station at three separate locations (“leapfrogging”) to cover the entire project area. These locations were co-registered to the local datum by resurveying several control points in the area of overlap from each base setup. This information was then used to adjust coordinates so that the entire survey referenced a common datum.

Ground control points (GCPs) were marked with an approximately 3-foot-wide “X” of 5-inch stripes using spray chalk. Except for a few cases where these marks were deeply shadowed or set on highly reflective surfaces, these marks produced clearly visible control points in collected aerial photos. Points used in the final surface development were filtered to remove those having poor accuracy. All points used in the surface development had positional (3D) dilution of precision (*i.e.*, PDOP) values < 3.0 and mean horizontal root mean squared (HRMS) and vertical RMS (VRMS) values of 0.07 and 0.08, respectively (± 0.02 in both cases; 1σ).

Thalweg survey

Thalweg survey data were collected with a Topcon GTS 236W total station. Bed elevation and water depth were recorded to the nearest tenth of a foot at each surveyed point. Depth was measured on the side of a stadia rod, oriented parallel to stream flow. Survey of the thalweg was complicated by the presence of several discrete paths between some in-stream boulders. To provide consistency with measurements, the flow path with the largest estimated discharge was surveyed. The exception to this approach was if access to that point was overly hazardous, in which case the most significant safely accessible flow path was surveyed. Numerous thalweg locations were surveyed in areas where large flow splits span several geomorphic units with multiple distinct pathways for upstream fish migration.

Most of the channel was dominated by step pool morphology (Figure 3). In these areas, two or three points were typically surveyed to characterize each step-pool unit. One point defines the step crest elevation and water depth. An additional one or two points were measured within deep pool locations. Large boulders dominated pool bottoms and often created two to three feet of local relief on the pool bottoms, making determination of the exact deepest point infeasible. In areas of rapid or cascade morphology, points were selected to illustrate the general bed profile.

Drone Survey for Structure from Motion (SfM) and Orthomosaic

Nadir photographs of the project reach were acquired with a small, lightweight unmanned aircraft system (sUAS). The sUAS employed was a DJI Phantom 4, equipped with the stock 12.4-megapixel camera.

The topographic surface extent (study reach) spanned from the Highway 14 road surface to the treeline on the south bank, extending from approximately Mile Post (MP) 28 to 29 (approximate RKM 71-73, Figure 4). To maintain a relatively consistent altitude relative to the terrain, avoid obstacles such as trees, power lines, and mountain sides, and optimize sUAS battery time, the mission plan required flying the reach in 10 zones (Figure 4). Each zone was flown at an altitude approximately 240 feet above the channel; flight paths nominally provided 85 percent front overlap and 75 percent side overlap of images, with 50-90 images acquired per zone. This resulted in an image pixel size of 2.9 cm (1.1 in). Six zones were flown separately on September 25th and 26th at different times of day, to provide images with differing illumination and shade conditions.

South Fork Clearwater River MP 28 Hypothesized Velocity Barrier

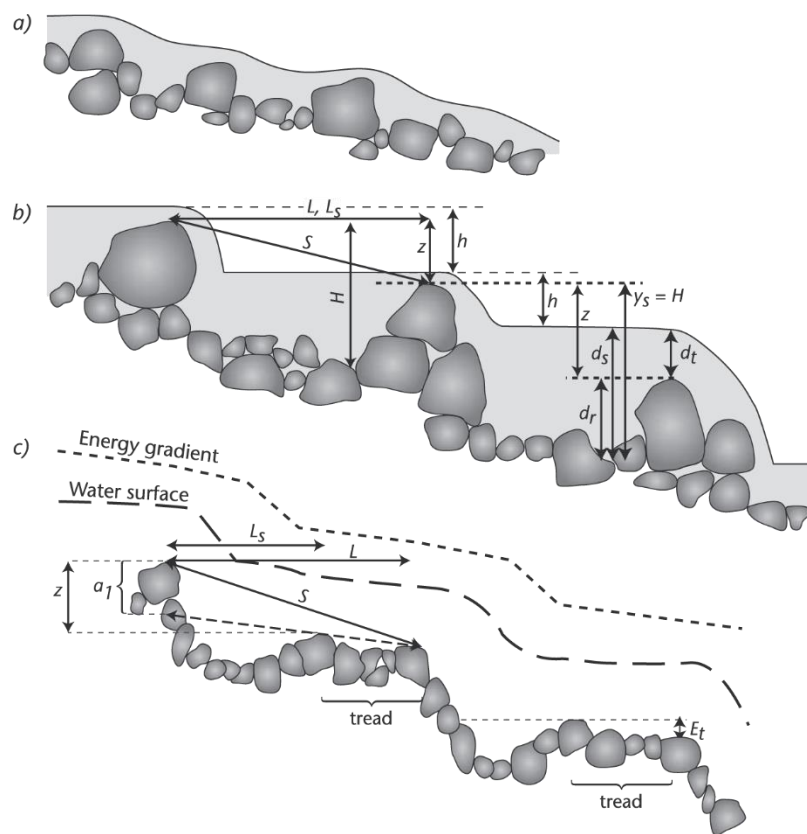


Figure 3. Examples of a) rapid, b) step-pool, and c) step-pool with tread channel morphologies. Adapted from Church and Zimmerman (2007).

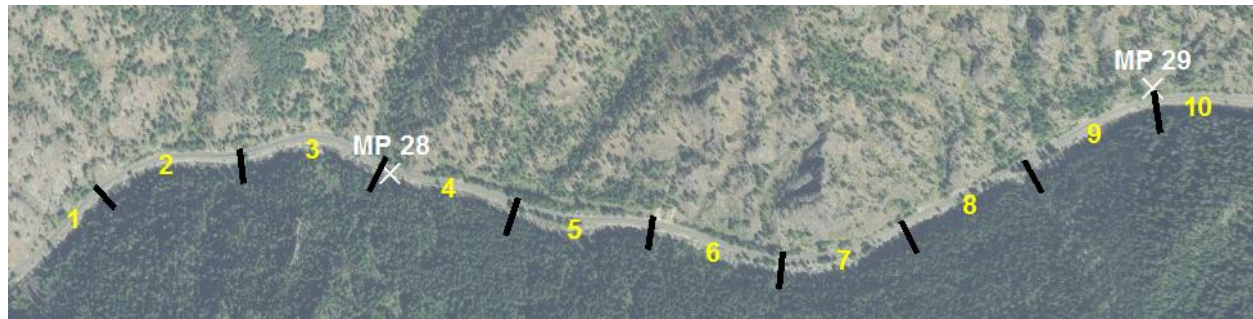


Figure 4. Study reach segmented by drone survey zones.

Data Processing and Surface Development

Structure from Motion Digital Surface Model Development

The terrain surface was built using a photogrammetric method called Structure from Motion (SfM). SfM is a computer vision-based workflow in which sets of high resolution overlapping images are processed to determine camera orientation and pixel coordinates. This information is then put in real coordinate space by using image-to-image registration methods. The calculated relationships are used to create three-dimensional models that can subsequently be used to

orthorectify the images and create orthomosaics. For the current analyses, nadir images were processed using Pix4Dmapper Pro (Pix4D 2016), a commercial SfM photogrammetry program.

The completed point cloud, DSM, and orthomosaic were transformed from model coordinates to the local datum using the surveyed ground control points. Of the 57 surveyed points, 26 were used to transform the model to real-world coordinates, and 31 were used as validation points, which were used to quantify distortion of the final terrain model relative to real-world coordinates. For reference, Appendix A provides a post-production report generated by Pix4D for the final DSM¹.

DEM Development

The DSM developed by PiX4D provided a highly-detailed representation of the ground surface that was above the water surface and unobscured by vegetation. Further processing was necessary to develop a DEM of the ground surface and submerged channel bathymetry for purposes of hydraulic model development. Four data sources were integrated in this process: The DSM described above, (which was generalized to 10 cm (3.9 in) pixel size), the thalweg survey data, LiDAR data, and the USGS 10m DEM.

Discharge during the survey (estimated 74 cfs at the project site) was low compared to the range of target flows for the hydraulic model (~300-3,200 cfs). The elevation difference between water surface and the stream bed at step crests was determined to be hydraulically insignificant, and because of this, bed elevation in these areas were defined by water-surface topography. In contrast, the offset between water surface and bed elevation is much larger in pools; the resulting slower velocities may provide key resting places for migrating fish, making it important to explicitly represent these areas in the hydraulic model. The first step in the creation of the DEM, therefore, was to impose pool areas into the DSM. Pools were added to the bathymetry by creating polygons that represented their extent on the aerial photo Orthomosaic. Bed elevations were added to the polygons using surveyed points and interpretation of depth from the aerial photo. Next, bed geometry was interpolated into the surrounding DSM at the margins of the pool feature.

Vegetation that obscured areas outside of the channel was replaced using LiDAR data (QSI 2015) that had been resampled to match the DSM pixel size. Remaining areas within the channel where vegetation or other obstructions (such as log bridges between boulders) distorted the surface were removed by masking and then replaced with elevations interpolated from the surface across the problem area.

For areas beyond the extent of the available LiDAR data, surface elevation was interpolated from channel margins and upslope contours derived from the 10m DEM.

¹ Surface pixel size, or ground sampling distance, for the report in Appendix A is 1.1 inches, and the composite root mean square error of the surface is 1.9 inches.

Hydraulic and Hydrologic Analyses

Hydrology

Existing/Historical Conditions

Available Data

Fish passage opportunities within the project reach are governed in part by stream flow (insofar as flow affects velocities and turbulence); therefore, determining the range of flows expected at the project site is a critical first step. While the project site is un-gaged, recorded stream flows are plentiful elsewhere on the SF Clearwater River. The USGS operates, or has operated, three gages with flows relevant to those at the project site: “SF Clearwater River at Stites” (Gage 13338500); “SF Clearwater River near Grangeville” (Gage 13338000); and “SF Clearwater River near Elk City” (Gage 13337500). These gages have drainage areas of 1168, 839, and 261 mi², respectively, similar periods of record, and are located as shown on Figure 5. Note the project reach is located between the gages near Grangeville and Elk City, with a drainage area of 498 mi².

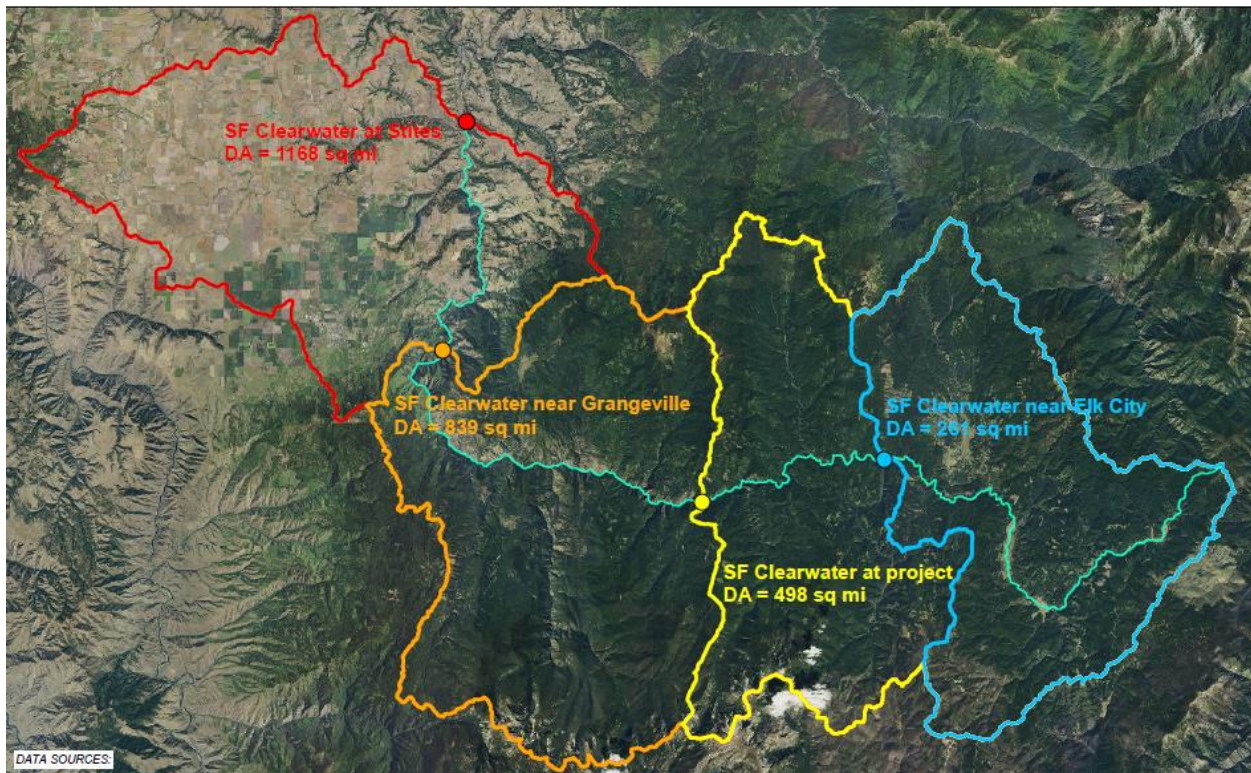


Figure 5. Locations of USGS gages and boundaries for contributing watersheds along the SF Clearwater River, relative to the project site. Blue, orange, and red lines and points indicate watershed boundaries and location of USGS gages near Elk City, Grangeville, and Stites, respectively. Yellow line indicates watershed contributing to discharge at the study reach in addition to in-stream flow measured at the Elk City gage. Yellow point indicates project site.

Flood Frequency Assessment

Standard recurrence interval flows at the project site were assigned by first computing flood frequency curves for annual maximum flows at the Elk City and Grangeville sites, and then transposing standard quantiles to the project reach. Flood frequency analysis was performed on the annual peaks at the gaged sites using a log-Pearson type III distribution, following procedures outlined in Bulletin 17B (USGS 1982). Statistical procedures to compute station skew, apply weighting using a regional skew, detect and treat high and low outliers, and determine confidence limits are explicitly stated in Bulletin 17B. The computations were performed using HEC-SSP (Brunner and Fleming 2010), a software program developed by the U.S. Army Corps of Engineers (USACE) for performing statistical analyses of hydrologic data.

Flow Duration

Annual flow duration at the project site was computed for the period of record common to the Elk City and Grangeville gages (WY 1945-1963) after interpolating between the mean daily flows by drainage area. The resulting curve was compared to flow duration curves computed by transposing the full period of record at each gage to the project reach, and scaling for drainage area, following the procedure recommended by Berenbrock (2002).

On this basis, a relationship equating daily flow at the project site to 1.73 times the flow at the Elk City gage was determined. The three curves were similar, with the curve for the common period of record generally falling between the others, as displayed in Figure 6. Note the 1 percent and 10 percent chance exceedance flows are 3,180 cfs and 1,650 cfs, respectively. Scaled daily flows from the Elk City gage were used to develop an annual hydrograph at the project site with percent exceedance curves. In addition, the relationship between flow at the Elk City gage and project site was used to evaluate daily exceedance percentiles and estimate a project site flow of 74 cfs flow during the field survey.

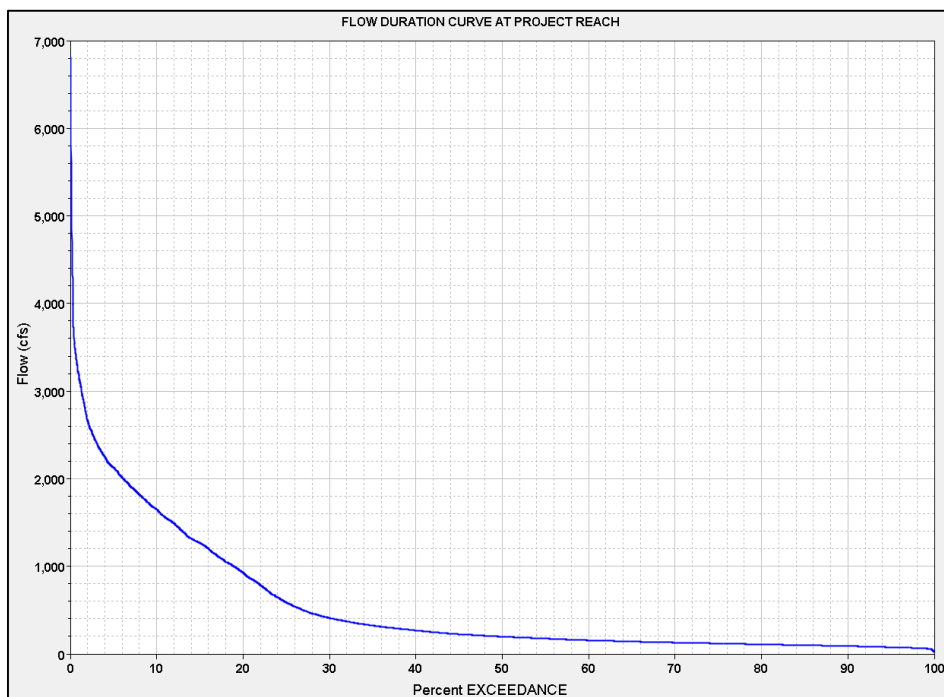


Figure 6. Scaled flow exceedance curve evaluated for the project site.

Climate Change Impacts

The Climate Impacts Group (CIG) at the University of Washington developed a physically based hydrologic model (the Variable Infiltration Capacity, or VIC model) for the Columbia basin, which is driven by climatic inputs of temperature and precipitation to represent scenarios of future climate (CIG 2010). The simulated daily stream flows were analyzed to determine peak flow frequency by fitting a generalized extreme value (GEV) distribution (CIG 2010). Flows at this project location were not separately analyzed by CIG (CIG 2010); however, flows corresponding to the larger Clearwater River basin at Orofino were analyzed and summarized here. Also summarized are the 2010 CIG results for two basins with a drainage area more similar to that of the project area: the Lochsa River and Selway River, both near Lowell, ID (approximately 23 miles East of Kooskia, ID). The basic geographic characteristics of these “analog” watersheds are given in Table 1.

It is important to note that results for the project area may differ considerably from the analog watersheds due to local basin influences, such as watershed hypsometry (elevation) and aspect (which both affect snow accumulation and melt), and river network configurations (which affects peak flow dynamics and magnitude). Nevertheless, the statistical analysis of forecasted project stream flows is beyond the scope of the present project, and the results summarized here for the alternate watersheds provide at least an indication of the qualitative changes expected for the region.

Furthermore, uncertainty associated with estimates of future peak flows is high. While there is a need to provide quantitative information for water resources and flood protection planning, the underlying projections of climate change are subject to large and unquantifiable uncertainty. The main unknown sources are future emissions of greenhouse gases; the uncertain response of the global climate system to increases in greenhouse gas concentrations; and incomplete understanding of regional manifestations that will result from global changes (Hawkins and Sutton 2011). Application of the hydrologic model and downscaling — both in space and time — of GCM-projected climate variables, represent additional sources of uncertainty. Hydrologic projections should be considered plausible representations of the future, given the best current scientific information, and do not represent specific predictions.

Table 1. Summary of basin characteristics for project area and gages used for hydrologic analysis.

Basin Characteristic	Project Area	Clearwater at Elk City	Clearwater at Orofino	Lochsa near Lowell	Selway near Lowell
Area (mi ²)	498	261	5,507	1,178	1,915
Mean Elevation (ft)	5,200	5,090	4,740	5,200	5,520
Mean Precipitation (in)	35.4	35.2	37.4	46.7	40.6
Forest Cover (%)	92	92	77	88	82
Mean Basin Slope (%)	28	25	34	38	44

* Note: Basin area as reported by USGS attributes for each gage, and by USGS StreamStats (V3) for project location. Remaining attributes as reported by USGS StreamStats for all locations.

Hydraulics

Model Development

Hydraulic conditions on the SF Clearwater River at and around the suspected fish passage barrier were computed using the two-dimensional (2D) capabilities of HEC-RAS software (USACE 2016). The model solves the 2D unsteady flow equations using an implicit finite volume algorithm and returns depth-averaged hydraulic properties such as depth, velocity, and shear stress. The final composite terrain was imported into HEC-RAS to define the river bed and surrounding topography. The modeled domain was one reach with a single upstream inflow and a one downstream outflow. No breaklines were included, as the project area has no special hydraulic structures such as bridges, culverts, or weirs. A single cell size (described below) was assigned to the entire domain. Three hydraulic roughness zones were delineated representing the channel, steep side banks, and roadway surface. The modeled domain encompassed the highway to the south bank and extended approximately 3,800 feet (MP 28.15 to 28.85). The modeled reach was a subset of the entire topographic surface, in part to reduce computation time and to restrict the modeled area to the extent of the thalweg survey. Figure 7 illustrates the modeled domain.

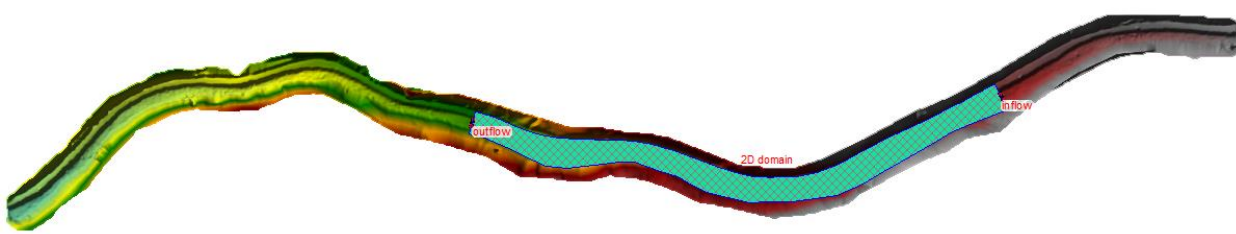


Figure 7. Complete DEM with hydraulic model domain highlighted.

Sensitivity Analysis

The model's sensitivity to several parameters was evaluated to quantify their impact on the final solution and provide context when evaluating fish metrics within the river. Model sensitivity was especially important because of limited data available to calibrate or validate the model. Five parameters were evaluated: solution equations, cell size, solution time step, roughness coefficient, and turbulence coefficient.

Solution equations

The model was initially solved using the full momentum and the diffusion wave equations, holding all other variables constant, in order to confirm which was most applicable. It was quickly apparent that the full momentum equations were critical in this application, because they account for local acceleration and convective acceleration terms that are impactful in the project reach. The extremely large ($D_{84} = 8$ ft) and abundant boulders on the riverbed form significant obstructions, forcing dendritic flow paths and areas of local acceleration as water spills from pools, over steps, and back into pools (subcritical regime, to supercritical, and back to subcritical).

South Fork Clearwater River MP 28 Hypothesized Velocity Barrier

Cell size

A proper cell size was also critical for computing local hydraulics and subsequently evaluating a fish's ability to navigate through and/or hold within the river. Nominally square computation cells were evaluated at 9, 6, 3, 2, and 1 foot in size, which ranged from the approximate D_{90} to less than the D_{10} of boulder roughness elements in the channel. Cell size was reduced until the optimum between maximizing numerical accuracy and minimizing computation time was identified. Tests were performed at discharges of 74 cfs (approximate flow at the study reach during survey) and 1,150 cfs (approximate mean annual flow) while holding all other parameters constant (except the time step which was reduced as appropriate). Figure 8 illustrates this balance. Smaller cells were found to better simulate hydraulic form losses, steep water slope, and dendritic flow paths, resulting in a correspondingly higher water surface. The graphic illustrates that a point of diminishing return was achieved at a mesh cell size of two feet, therefore this cell size was selected for evaluating fish passage.

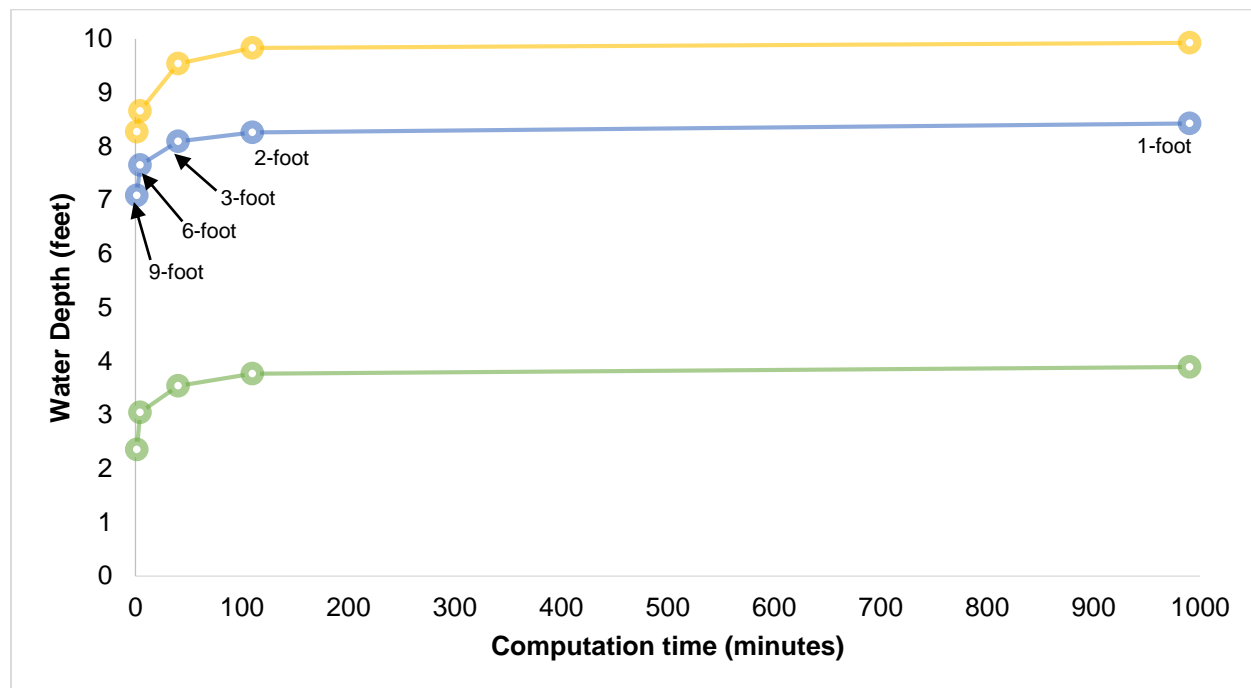


Figure 8. Computed water depth vs. computation time at three locations above the Snagging Hole with $Q_w=1,150$ cfs.

South Fork Clearwater River MP 28 Hypothesized Velocity Barrier

Figure 9 depicts the scale of the 2-foot computational grid in relation to the typical streambed substrate, showing how the model is capable of explicitly evaluating and representing flow through slots between boulders.

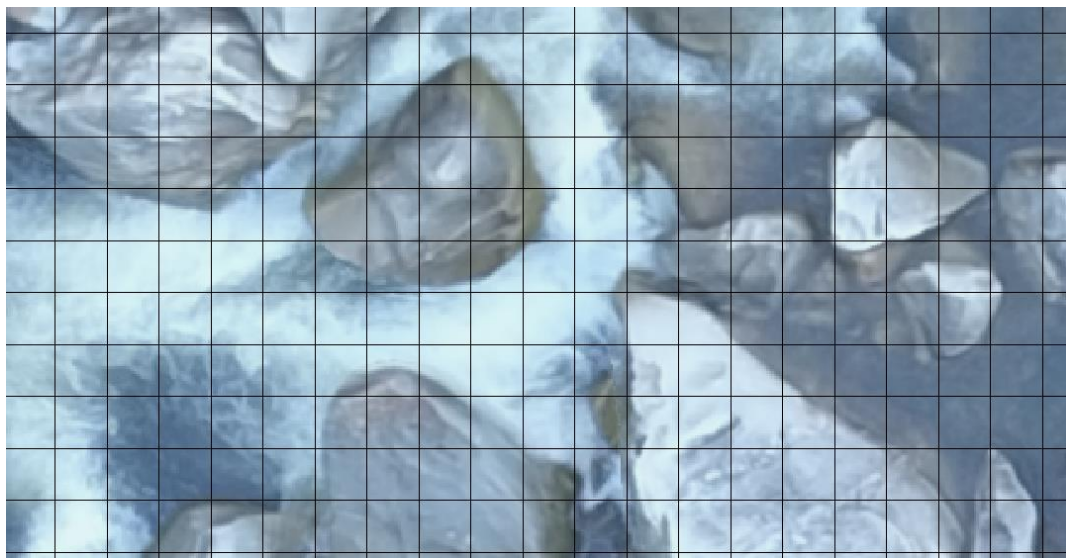


Figure 9. 2-foot grid overlying scaled image of typical streambed in the study reach, showing relation of computational cells to local topography forced by boulders.

Solution time step

Next, the time step used for modeling was evaluated to ensure use of an appropriate value for the selected computational mesh. In general, an adequate time step is a function of the cell size and velocity of the flow moving through the cells. At 74 and 1,150 cfs, the time steps evaluated were shown to impact the computed water surface solution by less than 0.1 feet. The time step used in the final simulations was 0.1 seconds ensuring a Courant number (the portion of a cell that a particle or solute will traverse by bulk flow transport in one time step) of 1.0 or less, meaning fluid particles move from one cell to another within, at most, a single time step.

Roughness coefficient

The roughness coefficient (Manning's n) in the model also impacts the computed solution. Lacking clear calibration information, sensitivity of the solution with respect to Manning's n was tested. Three roughness zones were delineated representing the channel, steep side banks, and roadway surface². Abundant literature exists documenting proper selection of Manning's n , but little of it evaluates steep ($>3\%$) boulder strewn rivers, and much less of it applies to two-dimensional models. Initial roughness selection was based on equations in three publications (Chow 1959; Jarrett 1985; Soto and Madrid-Aris 1994). The equations compute roughness as various functions of slope, hydraulic radius, dominant grain size, Froude number, and Chow's

² In the range of flows simulated, the river never crested the road; thus, Manning's n for the road was irrelevant to modeled in-stream hydraulics.

South Fork Clearwater River MP 28 Hypothesized Velocity Barrier

qualitative assessments of the river course. Using these three publications, roughness coefficients ranging from 0.1 to 0.18 were computed at five locations between Birdhouse and Snagging Hole at mean annual flow. Note that all three publications compute roughness for one-dimensional (1D) models. However, Morvan et. al (2008) state that 2D models should not necessarily use the same friction factor as 1D models because it is accounting for fewer losses in 2D models.

Therefore, sensitivity of the computed solution was carried out on Manning's n values of 0.04, 0.06, 0.08, 0.1, and 0.12 at flows of 74 cfs, 1,150 cfs and 3,190 cfs. Figure 10 illustrates the difference in computed water surface elevation and velocity extending 150 feet above Snagging Hole, holding all other variables constant. A change in roughness of 0.02 translates to an approximate 0.2-foot change in water surface (which is most pronounced below steps and on the upstream side of pools, where flow transitions from supercritical to subcritical regime). The same roughness coefficient change typically translates to a change in velocity of 1 fps, which is most pronounced at steps. The Manning's n used in the final simulations for evaluating fish passage was 0.08. This was chosen in part because it is slightly less than the range of values computed with the 1D roughness publications; in part because it is the median of the five values tested, making an expected range of plausible hydraulic conditions easier to quantify and because of the model validation results.

South Fork Clearwater River MP 28 Hypothesized Velocity Barrier

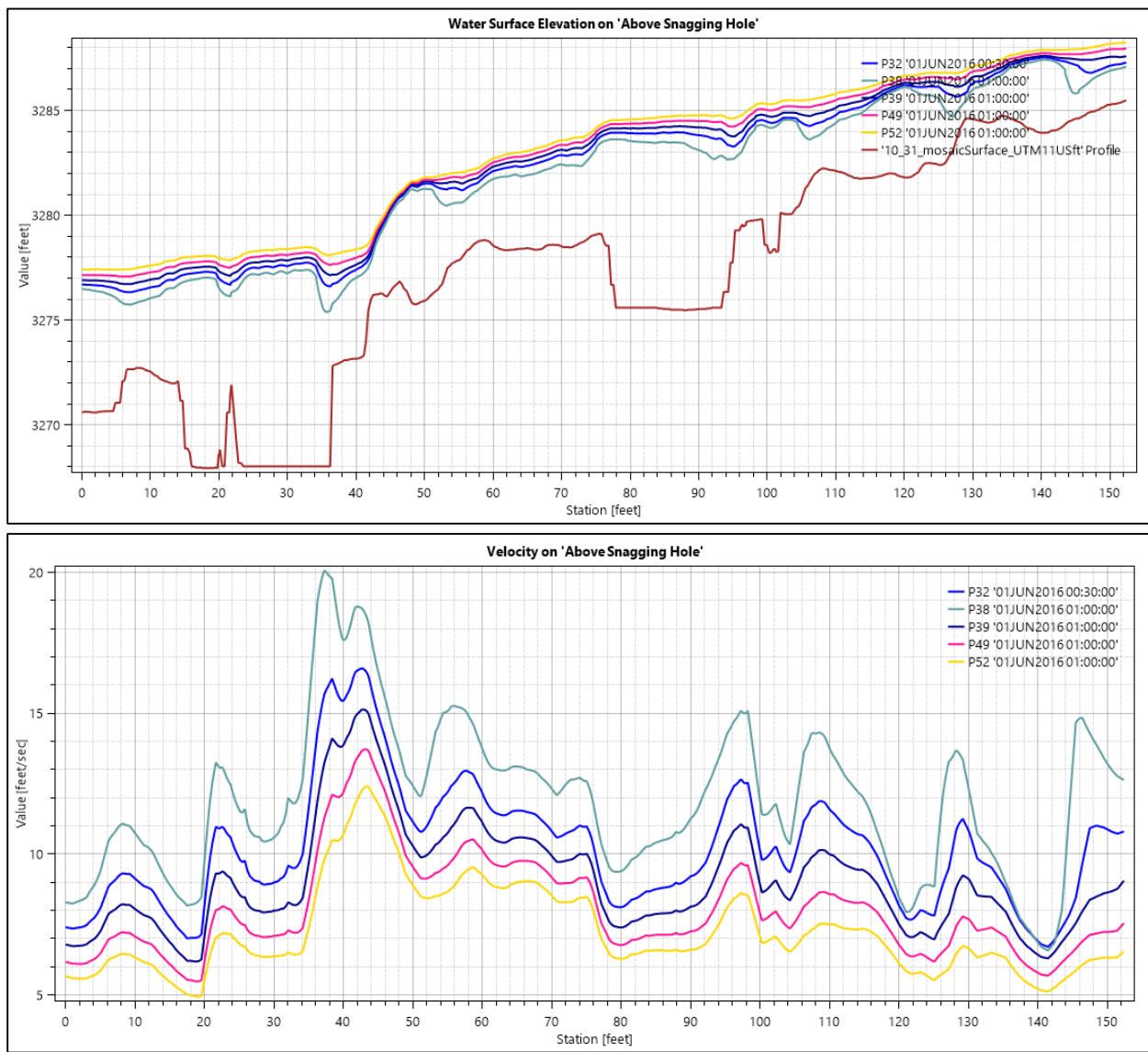


Figure 10. Computed water surface elevation (top) and velocity (bottom) with varying roughness coefficient (Manning's n). P38 was computed with $n=0.04$, P32 with $n=0.06$, P39 with $n=0.08$, P49 with $n=0.1$ and P52 with $n=0.12$.

Turbulence coefficient

HEC-RAS offers the ability to include increasing effects of turbulence in the flow field, as well as those effects inherent to the full momentum equations. The SF Clearwater River is a highly turbulent river and therefore the impact of increasing the turbulence coefficient was also tested. The HEC-RAS user's manual provides a range of turbulence coefficients and their qualitative expected mixing intensity. The use of the high values, describing turbulence observed in rough surfaces and strong meanders, was found to be stable at low flows, but less so at higher discharges and higher roughness coefficients. In general, the impact of the turbulence coefficient

South Fork Clearwater River MP 28 Hypothesized Velocity Barrier

was similar in magnitude and direction to increasing the Manning's n by 0.02 (i.e. the water depth with a Manning's n of 0.06, with additional turbulence was similar to that with a Manning's n of 0.08 and no turbulence beyond that provided by the default numerical scheme in HEC-RAS). Because the turbulence factor tended to make simulations unstable, the final model parameterization did not leverage it.

Final Model Parameters

The model parameters tested for sensitivity and used in the final fish passage evaluation are summarized in Table 2.

Table 2. Final Model Parametrization.

<i>Model Parameter</i>	<i>Value</i>
<i>Solution Equations</i>	Full Momentum
<i>Cell Size</i>	2 ft (163,849 cells)
<i>Time Step</i>	0.1 s
<i>Manning's n</i>	0.08
<i>Viscosity Coefficient</i>	0

Model Validation

The model with the final parameterization described in Table 2 was then validated by comparing model results to empirical observations collected during the site survey and to select photos of the river at Snagging Hole provided by NPT, as described in the subsequent sections.

Survey Observations

The river's discharge during the survey was 43 ± 4 cfs at the Elk City gage, which transposed to the project reach, is approximately 74 cfs. Using the final modeled parameters, the computed wetted channel extent and relative velocity were compared to the observed conditions. Figure 11 illustrates close agreement between modeled flow inundation area and relative velocity when compared to field observations. Simulated pool depths were compared to those surveyed and also found in close agreement (Figure 12). Of the 250 thalweg points measured, 42 percent are within ± 0.5 feet of the simulated water depth and 72 percent are within ± 1.0 feet. The scatter shows bias towards under-simulating the depth, but this is more a reflection that not all surveyed thalweg points were forced into the final topographic surface; therefore, the simulated depth at these locations is not indicative of the river's true depth. Scatter is also due to the extreme variability inherent to measuring pool depth on the SF Clearwater River, where the pool bottom is highly irregular due to boulders and the water surface varies from turbulence.

 South Fork Clearwater River MP 28 Hypothesized Velocity Barrier

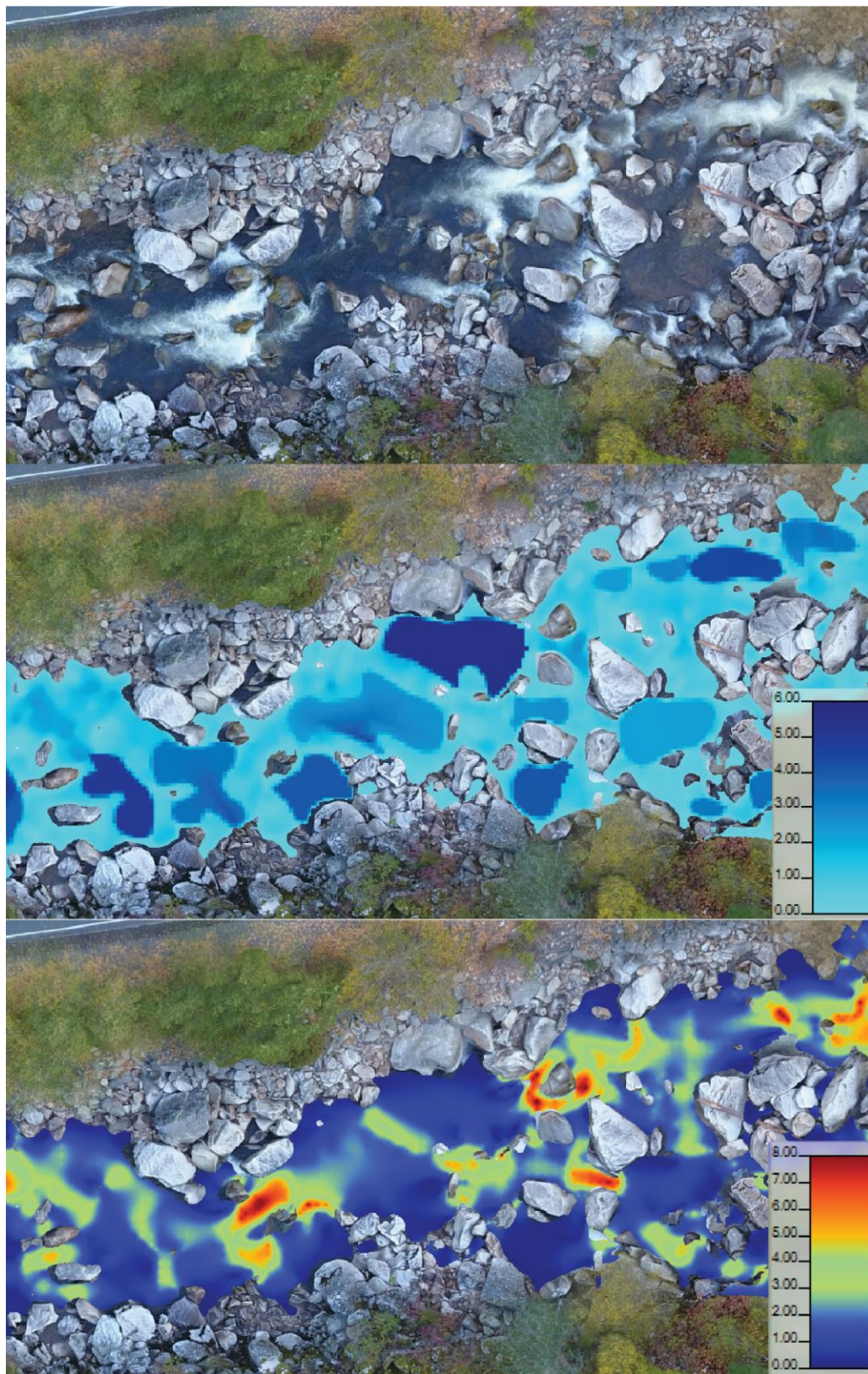


Figure 11. Orthophoto from time of survey (top), and modeled flow depth in feet (middle) and velocity in feet per second (bottom) for the same discharge.

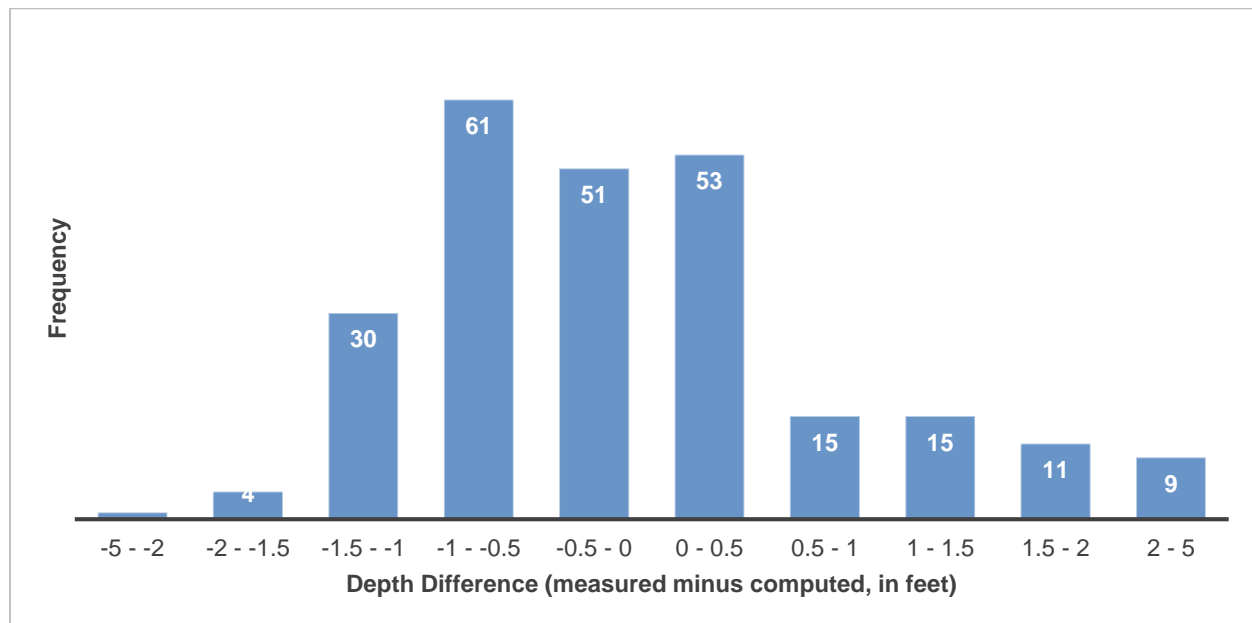


Figure 12. Frequency of occurrence of binned ranges of difference between measured and computed thalweg depth at $Q_w=74$ cfs. Note high degree of correlation, as evidence by the observation that 72% ($n=180$) of modeled thalweg depths were within ± 1 ft of surveyed depth measurements.

Photographs at Snagging Hole

NPT provided several photographs of the river taken from Snagging Hole for validation. Discharges corresponding to the five photos, transposed to the project reach, were 74, 625, 909, 999, and 1,074 cfs. Figure 13 compares a photo of the reach above Snagging Hole on May 5, 2016 (620 cfs at Elk City and 1,074 cfs at Snagging Hole), with the computed water surface elevation for a discharge of 1,110 cfs, viewed from the same perspective as the photo. The water surface in Figure 13 is colored to illustrate the steep drop in water surface from the pool just above Snagging Hole. Note the dry rocks in the photo are similarly dry in the model, providing more qualitative evidence that the model accurately replicates hydraulic conditions in the project reach.

Figure 14 shows a map view of the simulated model results at Snagging Hole for 1,100 cfs. While not quantitative, the figures qualitatively replicate the hydraulic conditions shown in Figure 13. Similar qualitative agreement was found between the model and an NPT supplied photograph at a discharge of 625 cfs. Based on the validated information, the model was considered to be appropriate for the application of fish passage models to assess the existence of a fish passage barrier.

 South Fork Clearwater River MP 28 Hypothesized Velocity Barrier

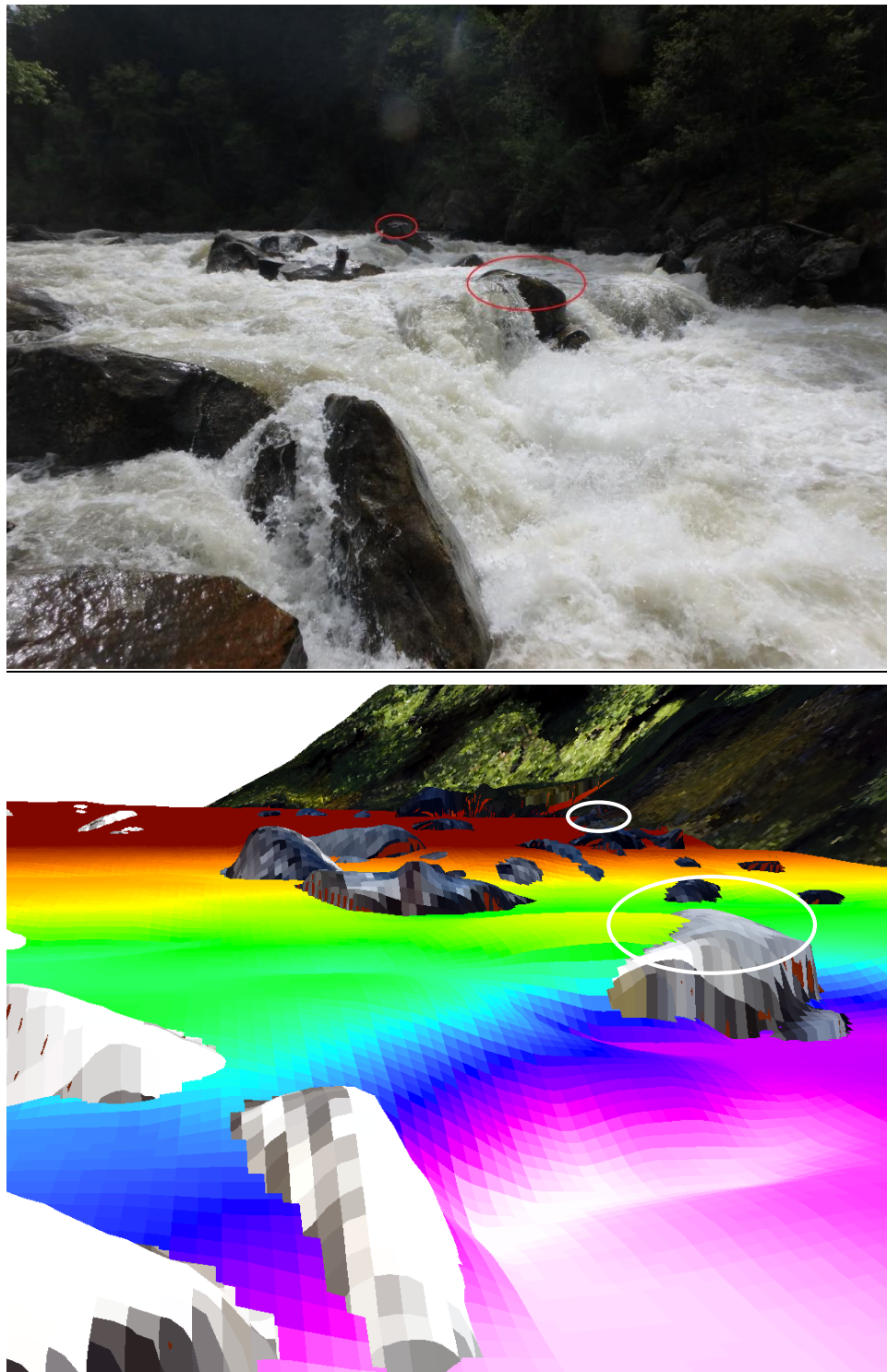


Figure 13. Comparison of photo (top) and model results (bottom) for the reach upstream from Snagging Hole. Estimated flow in the photo is 1,074 cfs and modeled flow is 1,100 cfs.

 South Fork Clearwater River MP 28 Hypothesized Velocity Barrier

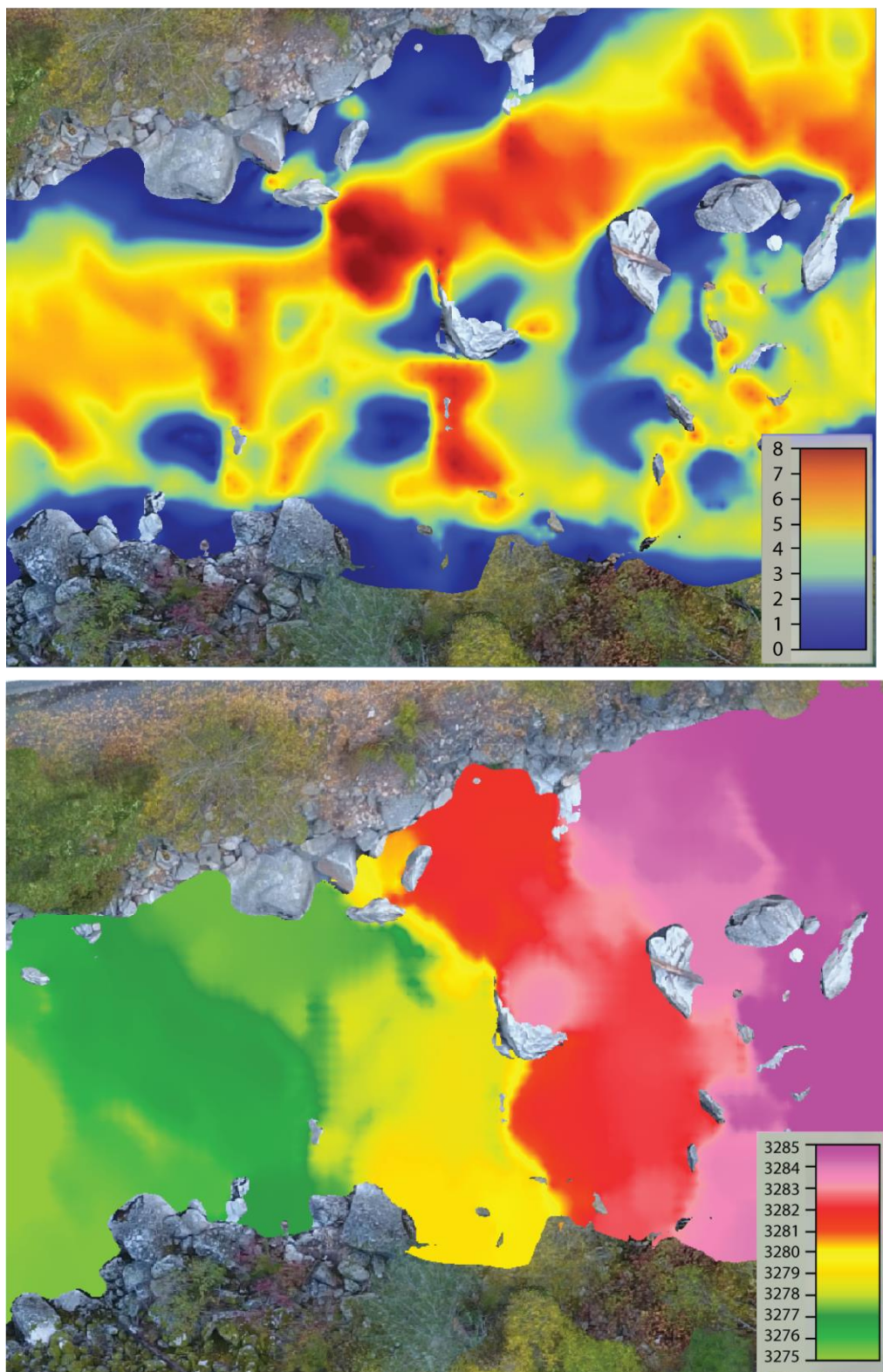


Figure 14. Modeled velocity (top, in feet per second) and water surface elevation (bottom, in ft above sea level) at Snagging Hole for a flow of 1,100 cfs.

Fish Contextualization

In this section, we discuss the ways in which the 2-D hydraulic modeling results are used to determine the effect of hydraulic conditions on the ability of steelhead to migrate through the study reach. The purpose of this section is to provide details of our approach to quantifying hydraulic conditions that exceed steelhead swimming burst speeds and durations. For this study, we follow the swim speed model developed by Hunter and Mayor (1986) to apply velocity criteria to the 2-D hydraulic modeling results (Equation 1). The model predicts the swimming speed of a steelhead and duration the fish is capable of sustaining that speed based a number of factors.

$$V = aL^b t^{-c} \quad (\text{Equation 1})$$

Where:

V = swim speed of fish relative to the water,

L = length of fish,

t = time to exhaustion, and

a , b , and c are regression coefficients (Hunter and Mayor 1986).

According to Idaho Fish and Game (IDFG 2016), Clearwater River “B-run” steelhead average approximately 80 cm. For the purposes of conservative modeling, here we estimate critical velocities for a steelhead with fork length of 90 cm (approximately 3 ft), similar to sizes of three ocean year fish returning to the Clearwater River. For a 90 cm steelhead, the coefficients are 12.3, 0.62, and -0.51 for a , b , and c respectively, yielding burst speeds of 2.5 m/s (20 s), 3.6 m/s (10 s), and 5.1 m/s (5 s). Note that this approach errs on the side of underestimating a barrier, *i.e.*, tending towards a false negative, while imparting results suggestive of a barrier with a higher degree of confidence.

In order to identify likely fish passage barriers, these predictions of burst speeds and durations must be evaluated in the context of instream flow velocities. As a general concept, the fish’s burst speed in the upstream (positive) direction (V_B) must overcome flow velocity in the downstream (negative) direction ($-V_W$), to yield net forward velocity of the fish (V_F ; Equation 2; Figure 15).

$$V_F = V_B + (-V_W) \quad (\text{Equation 2})$$

 South Fork Clearwater River MP 28 Hypothesized Velocity Barrier

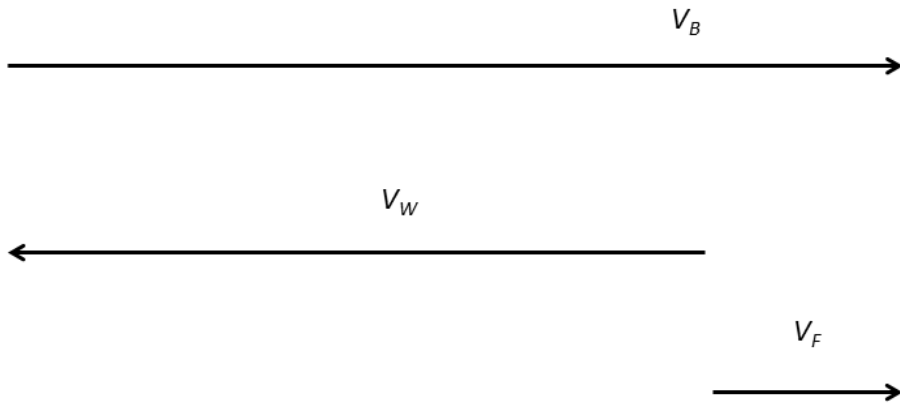


Figure 15. Conceptual diagram coupling a fish's upstream burst speed capability (V_B) with the downstream flow velocity (V_W). V_F represents the fish's actual upstream progress.

If $V_F < 0$ when a fish swims at maximum upstream burst velocity ($V_{B\text{crit}}$), then a barrier clearly exists for a given location. However, the duration that a fish can swim at burst speeds must also be taken into account: If $V_F > 0$, then a barrier still may exist if the length of the reach (L_{reach}) exhibiting velocity V_W is not passable in the duration of time that a fish can sustain a burst speed (t_{vb}) necessary to overcome flow velocity within the reach in question. Determining whether a reach of a given length is passable in an amount of time, given a swimming velocity, is a simple rate multiplication (*i.e.*, velocity times time equals distance). In this case, net upstream swimming velocity times the temporal duration a fish can sustain a burst swimming at the gross velocity required to generate that net upstream velocity. Thus, we formalize this set of passage rules as follows, with the explicit assumption that, if these conditions are *not* met, then a reach is passable:

FOR $V_B = V_{B\text{crit}}$:

IF $V_F < 0$,

THEN a barrier exists.

FOR ALL V_B :

IF the distance product $V_F \times t_{V_B} < L_{\text{reach}}$,

THEN a barrier exists.

Modeling Fish Burst Swimming Performance

One of the advantages of 2-D hydraulic modeling is that outputs are inherently spatial and include bed surface elevations, water depths, and velocities. Because these data are in grid format with 0.6 m (2 ft) resolution, it is possible to quantify the spatial connectivity and heterogeneity of important hydraulic parameters within river channels with a high level of detail that takes into account individual sediment clasts, hydraulic chutes, and pools. We calculated high resolution velocity grids for every 100 cfs increase in discharge, ranging from 100 cfs to 1500 cfs. For each grid, velocity values were classified into 4 groups that were determined by the Hunter and Mayor (1986) swimming speed model. Class breaks were determined as “non-burst swimming speed” (< 7.6 fps), “>20 Sec Burst Speed” (7.6 – 10.7 fps), “10 Sec Burst Speed” (10.8 fps – 15.3 fps), and “<5 Sec Burst Speed” (> 15.3 fps). For each of the 15 velocity grids, the polygons encompassing these four velocity classes were used to compute average velocities across all grid cells within each patch. It should be noted that one primary assumption of our approach was that fish encountering a patch of high velocity water were, in most cases, forced to attempt to traverse it due to obstructions such as large boulders or shallow depths in other parts of the channel.

In order to evaluate the distance a steelhead would have to swim through patches of velocity classes, we calculated the length of the patch’s mean axis. This length feeds back into equation 2 for all patches of V_w . Where these lengths exceed V_B , passage barriers exist under the criteria established in Hunter and Mayor (1986). All 15 of these grids were evaluated using equation 2 to determine if patches of velocity classes were large and intense enough to exceed a steelhead’s ability to migrate past each discrete patch in the study area and reach spawning habitat upstream.

Fish Behaviors Inferred from Tracking Data

During 21 September 2015 – 12 March 2016, 120 immigrating adult Steelhead were implanted with PIT tags and radio telemetry (RT) transmitters. This group comprises 91 fish that were tagged by the National Oceanic and Atmospheric Administration and Idaho Fish and Game staff at Lower Granite Dam (LGD) between 9/5/2015 and 10/28/2015. An additional 29 steelhead were tagged with RT transmitters between 2/12/2016 and 3/15/2016 in the South Fork Clearwater River downstream of the study area by NPT personnel. Steelhead were subsequently detected by NPT staff in 2016 using a combination of fixed RT receivers located along the SF Clearwater River and mobile RT receivers operated from vehicles traversing the bank of the SF Clearwater River above SF Clearwater RKM 55 (RKM 922 from the Pacific Ocean). Of this group of 199 steelhead, 24 fish (20%) were detected above Johns Creek, and thus within the study area (*i.e.*, they were available to attempt to pass the hypothesized barrier at ID-14 Mile Post 28, located at approximately SF Clearwater RKM 71 (RKM 938 from the Pacific Ocean).

Three (3) fixed RT antennas collected data 24 hrs per day between 1 February and 29 May 2016. The diel temporal distribution of detections within was visualized by plotting a histogram of hourly detection frequencies, to test for evidence of more or less active periods within a day for immigrating adult Steelhead (Figure 27 below).

Mobile tracking was also undertaken one (1) time per week between 8 March and 14 June 2016. Mobile tracking efforts involved driving along a 30-mile vehicle survey track during a constrained time period, generally during 09:00 – 14:00 (Figure 27 below). Mobile tracking

South Fork Clearwater River MP 28 Hypothesized Velocity Barrier

occurred in a systematic fashion, targeting “index” style sites that were repeatedly surveyed at similar times each week. While a systematic design such as this can reveal important trends, it should be noted that this approach has potential to introduce both spatial and temporal bias into the data, due to a lack of randomization. No mobile tracking occurred during the peak detection hours (Figure 27 below).

Next, we evaluated relative proportions of fish that successfully passed the hypothesized barrier, fish that entered the study area but did not pass (inferred to be an unsuccessful passage attempt), and fish that were not detected in the study area.

We assigned daily discharges from the USGS gage at Elk City (13337500) to each of the dates of highest upstream detection per fish, and to the dates of first detection upstream for fish that passed the hypothesized barrier. In order to visualize seasonal timing patterns associated with Steelhead spawning arrival and regional hydrology, we plotted the time series of numbers of fish detected and regional discharge on a single set of axes.

We then evaluated whether the RT data support test whether some threshold discharge prevents fish from passing the hypothesized barrier. To do this, we evaluated the range of mean daily discharge on the date of the last detection downstream of the barrier and first detection upstream of the barrier for fish that successfully passed the hypothesized barrier. Although limited in statistical power, these data can be used to evaluate differences in discharge when fish could be inferred to be attempting to pass the hypothesized barrier.

Next, we compared fork length (FL) at the time of tagging (based on data provided by Peter Cleary, NPT), among fish that were inferred to have passed the velocity barrier, based on RT detections, and those that were not detected above the barrier, which we lumped together as “failing” fish (Figure 30 below). We explicitly assume size at tagging accurately represents size at return. A two-tailed t-test assuming equal variance among groups was conducted to assess statistical significance of the difference between Passing and Failing groups.

Finally, we explore the anecdotal record of a single fish (#128), to provide an exemplary detection history pattern associated with a fish that did successfully pass the hypothesized barrier (Figure 31 below).

RESULTS

Geomorphic, Fish Habitat, and Fish Passage Barrier Survey

Field Survey & Surface Development

The field survey confirmed that the suspected fish passage barrier occurs in an especially steep and confined segment of the channel where it passes over a knickpoint formed by an apparent rockfall-dam. General slopes for the reach typically range from 2 to 4%, but as the channel crosses the knickpoint, the average bed slope (measured from step-crest to step crest) ranges from 5 to 8%, excluding one particularly large step over which a 5-foot hydraulic drop was present (Figure 16).

A local constriction at the suspected barrier is less pronounced. Surrounding reaches upstream and downstream range in width from 40 to 100 ft, with typical widths of 50 to 80 ft. From Birdhouse Hole to Snagging Hole, the channel width ranges from 50 to 70 ft, except at one notable constriction, where a large boulder blocks the left half of the channel at approximately ID-14 MP 28.32 (SF Clearwater RKM 71), and confines the flow to a 35 ft wide chute. The channel increases in width from 50 ft at Snagging Hole to 90 ft at the tailout of a large upstream pool. Through the suspected barrier reach, large boulders block up to two-thirds of the total channel width to near the bankfull elevation, confining most of the discharge to narrow chute features.

Digital files, including two orthomosaics (created from flights with different sun positions) and the compiled digital elevation model, are a key project deliverable. The coverage extents and high resolution of the products (3 cm for the orthomosaics, 10 cm for the DEM), preclude effective display of the products in this format, although Figure 17 shows an example of the surface. Appendix B includes a complete orthomosaic, and Appendix C includes the complete merged DEM surface. It is important to note that pools were only imposed on the surface in the area of the thalweg survey, which extended approximately from MP 28.23 to 28.75.

 South Fork Clearwater River MP 28 Hypothesized Velocity Barrier

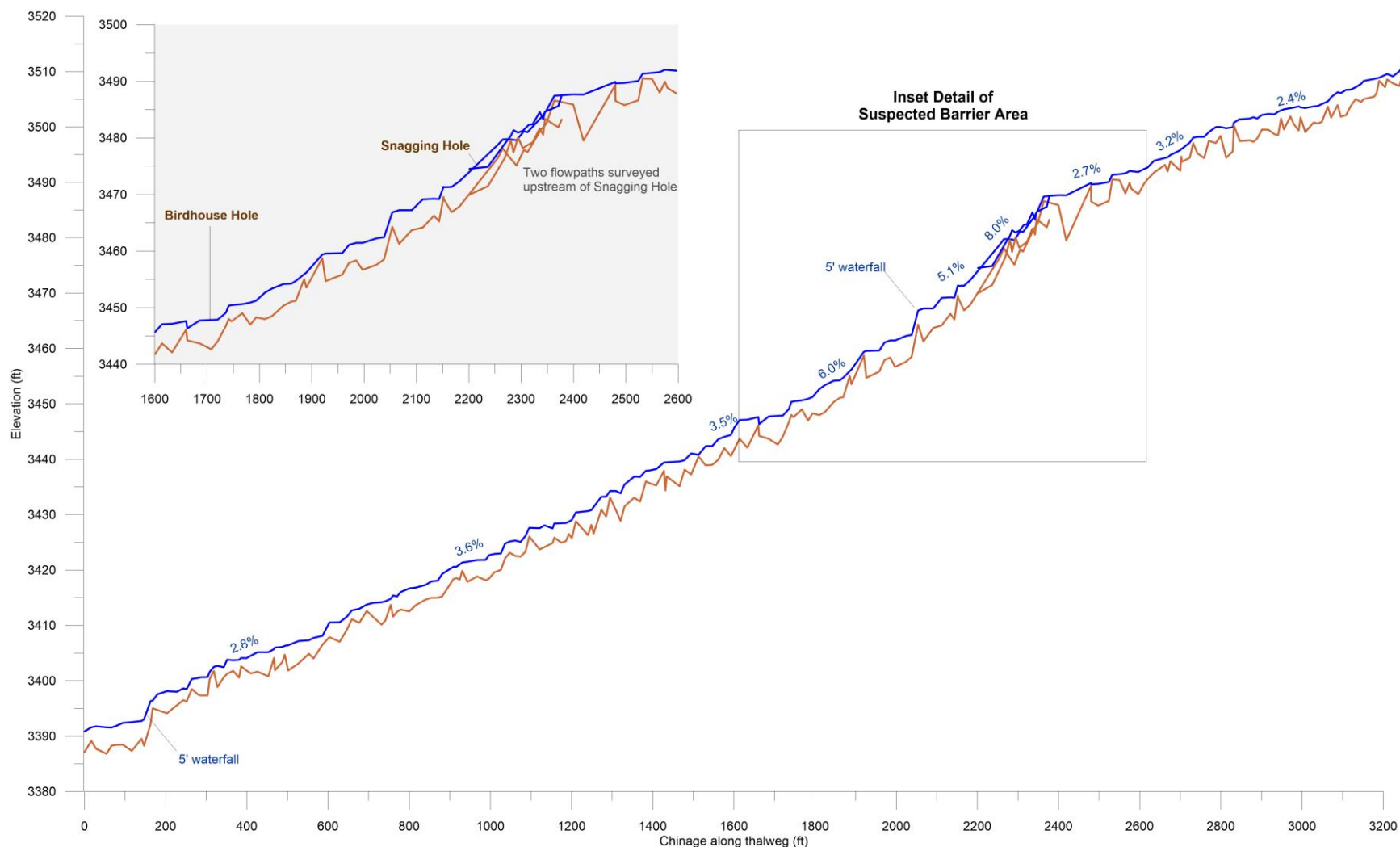


Figure 16. Surveyed thalweg and water surface profiles. Two sets of lines in the suspected barrier area reflect survey of two flow paths.

 South Fork Clearwater River MP 28 Hypothesized Velocity Barrier

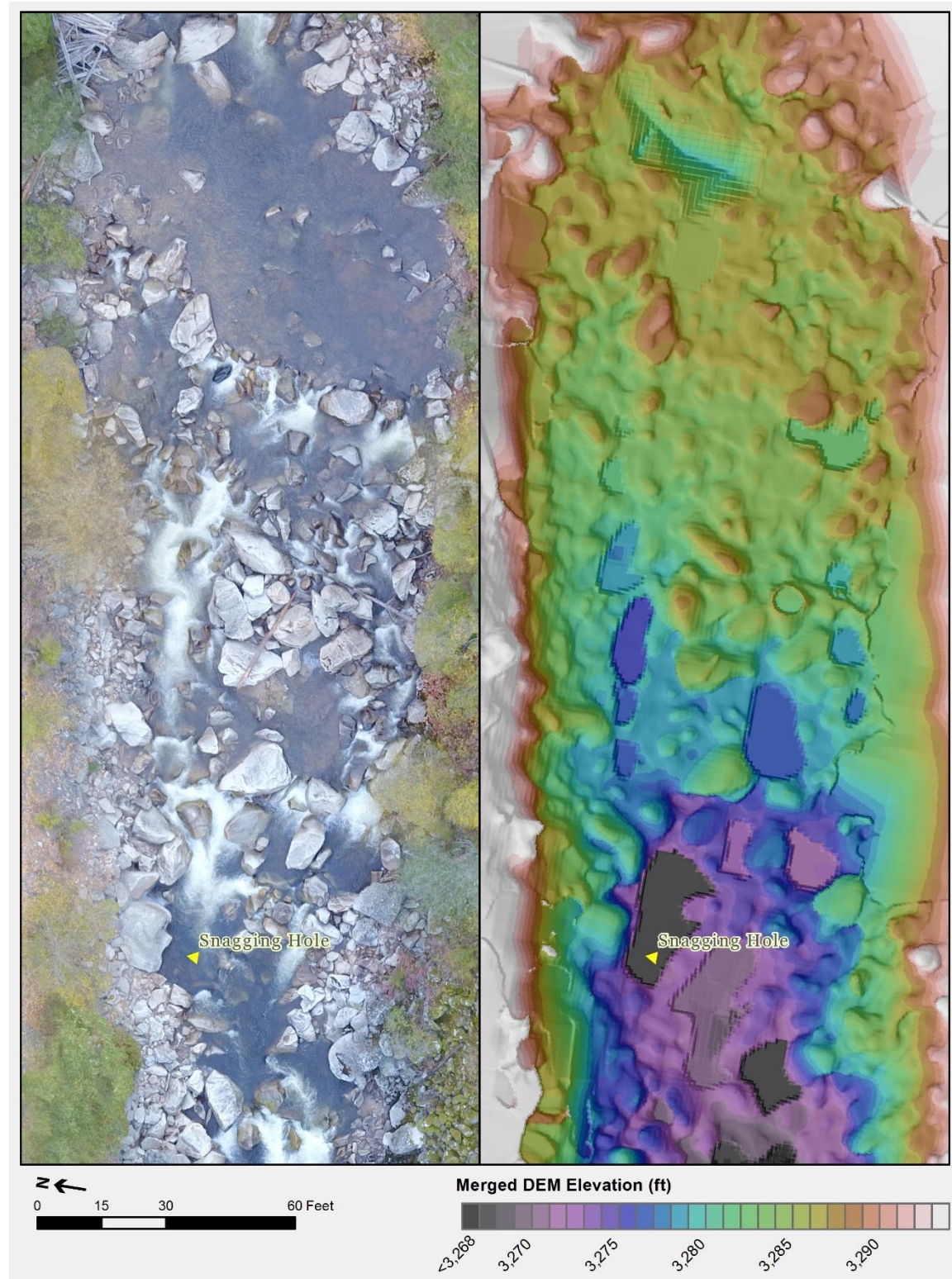


Figure 17. Example of native resolution orthophoto mosaic (left) and digital elevation model (right) developed from the sUAS survey. These images show the area from Snagging Hole to the deep pool upstream of the rockslide debris-dam.

Hydraulic and Hydrologic Analyses

Hydrology

Existing Conditions

Flood Frequency Assessment

Annual peak flows and fitted distribution are shown in Figure 18 and Figure 19. The computed curves fit the observed events well, with only one high outlier computed and one discharge falling outside the 95 percent confidence band (Gage 13338000). Computed station skews were weighted through use of gage-specific regional skews — identified on maps in Kjelstrom and Moffatt (1981) with a mean square error of 0.16 for rainfall-snowfall events (Berenbrock 2002).

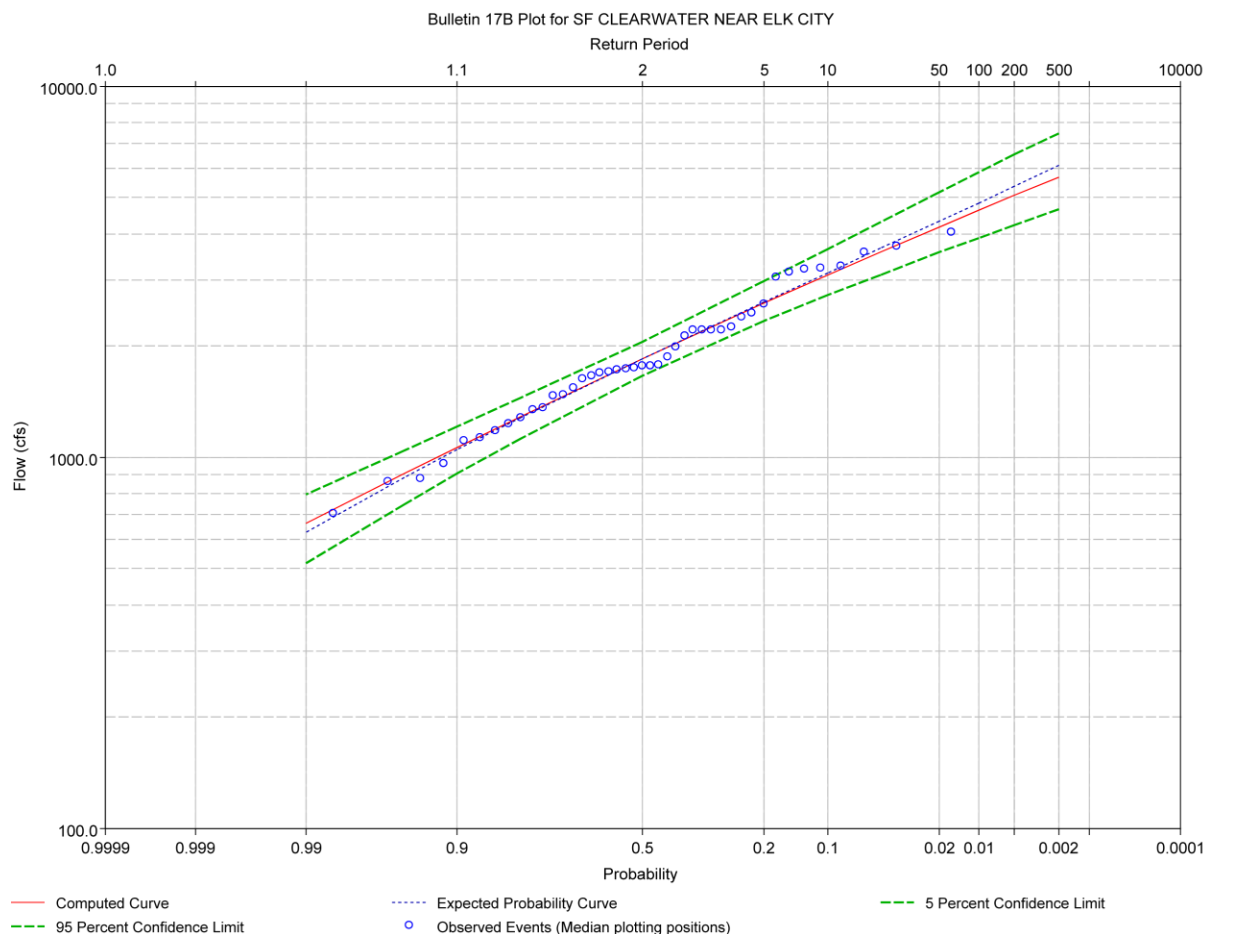


Figure 18. Annual peak flows and fitted distributions for the SF Clearwater River near Elk City.

South Fork Clearwater River MP 28 Hypothesized Velocity Barrier

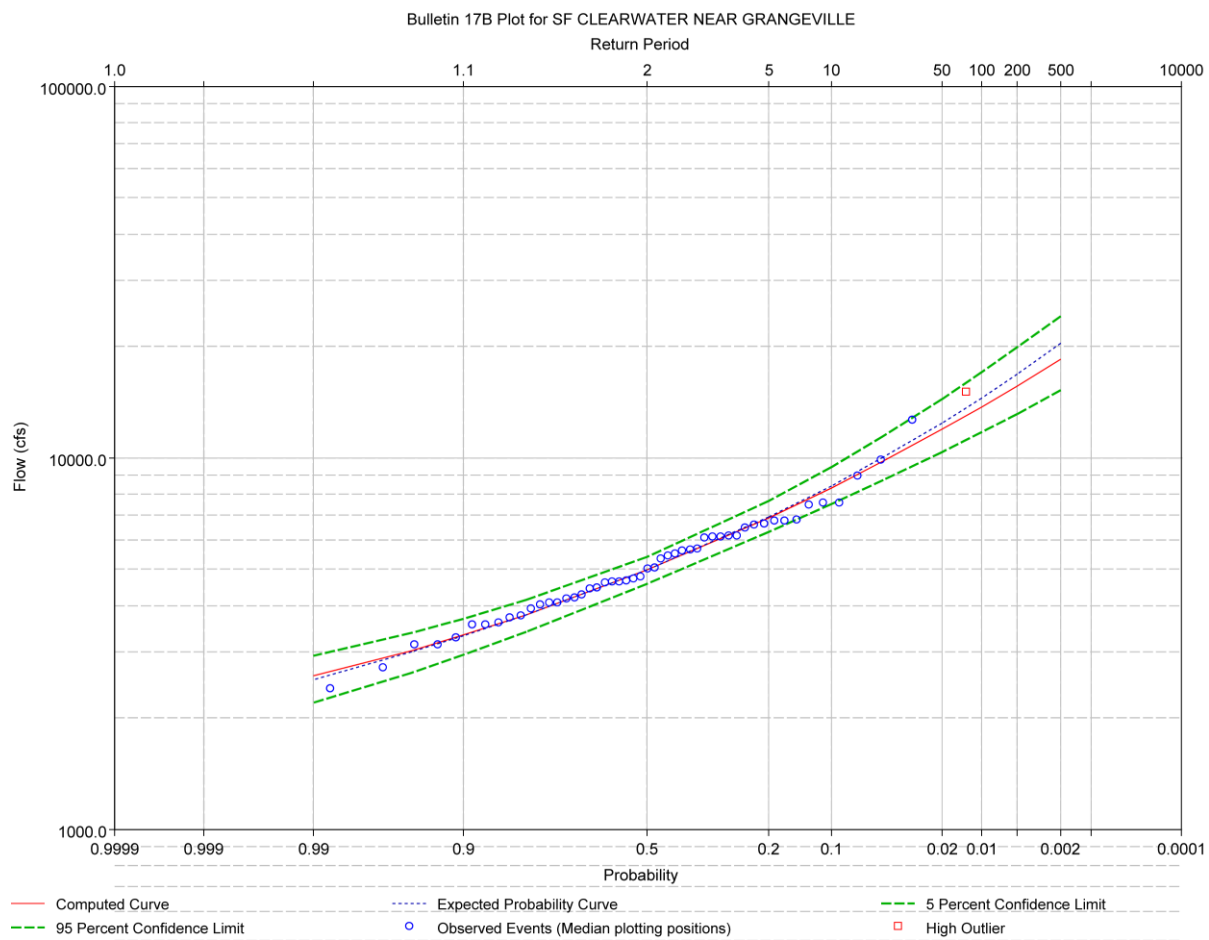


Figure 19. Annual peak flows and fitted distributions for the SF Clearwater River near Grangeville.

South Fork Clearwater River MP 28 Hypothesized Velocity Barrier

To determine frequency of occurrence and magnitude of frequent flood events within the project reach, flood quantiles at the project reach were estimated by interpolating between values for the Elk City and Grangeville gages (Berenbrock 2002). These interpolated flood quantiles range from an annual flow up to the 100-year return period are listed in Table 3. Flow within project reach (Q_{PR}) is estimated to be approximately 2x flow at the Elk city gage (Q_{EC}) across the range of flows expected within a five- year cycle (Table 3), although this relationship is non-linear with at least one inflection point near 2,000 cfs (Figure 20).

Table 3. Calculated flood discharges for adjacent USGS gages on the SF Clearwater River, interpolated flood discharges for the project site, and ratio between interpolated discharge for the project site and flow at the Elk City gage.

Return Period (years)	USGS “SF Clearwater near Grangeville” (cfs)	USGS “SF Clearwater near Elk City” (cfs)	Computed SF Clearwater at Project Reach (cfs)	$Q_{PR} : Q_{EC}$
100	13,689	4,629	8,344	1.80
50	11,919	4,176	7,351	1.76
25	9,783	3,570	6,118	1.71
10	8,292	3,098	5,228	1.69
5	6,874	2,601	4,353	1.67
2	4,981	1,842	3,129	1.70
1.01	2,580	662	1,449	2.19

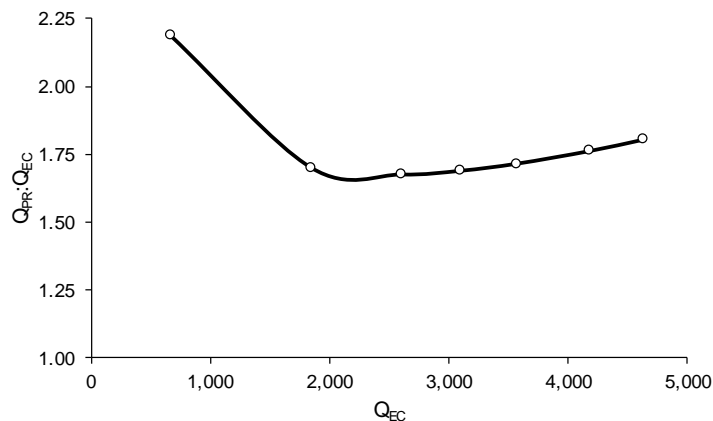


Figure 20. Ratio of computed flow in project reach (Q_{PR}) to flow at Elk City (Q_{EC}), across a range of Q_{EC} .

South Fork Clearwater River MP 28 Hypothesized Velocity Barrier

Daily Flows

Spring Migration for Steelhead on the SF Clearwater River coincides with the spring snowmelt flood (freshet) between March and June. The annual flood peak normally occurs during this period, and, as described above, typically ranges from approximately 1,500 to more than 5,000 cfs. A raster hydrograph (Figure 21) illustrates daily flows for the entire period of record. The freshet flood period typically lasts about 3.5 months, but flows above 1,000 cfs rarely occur for periods longer than two weeks, at most persisting for up to approximately one month.

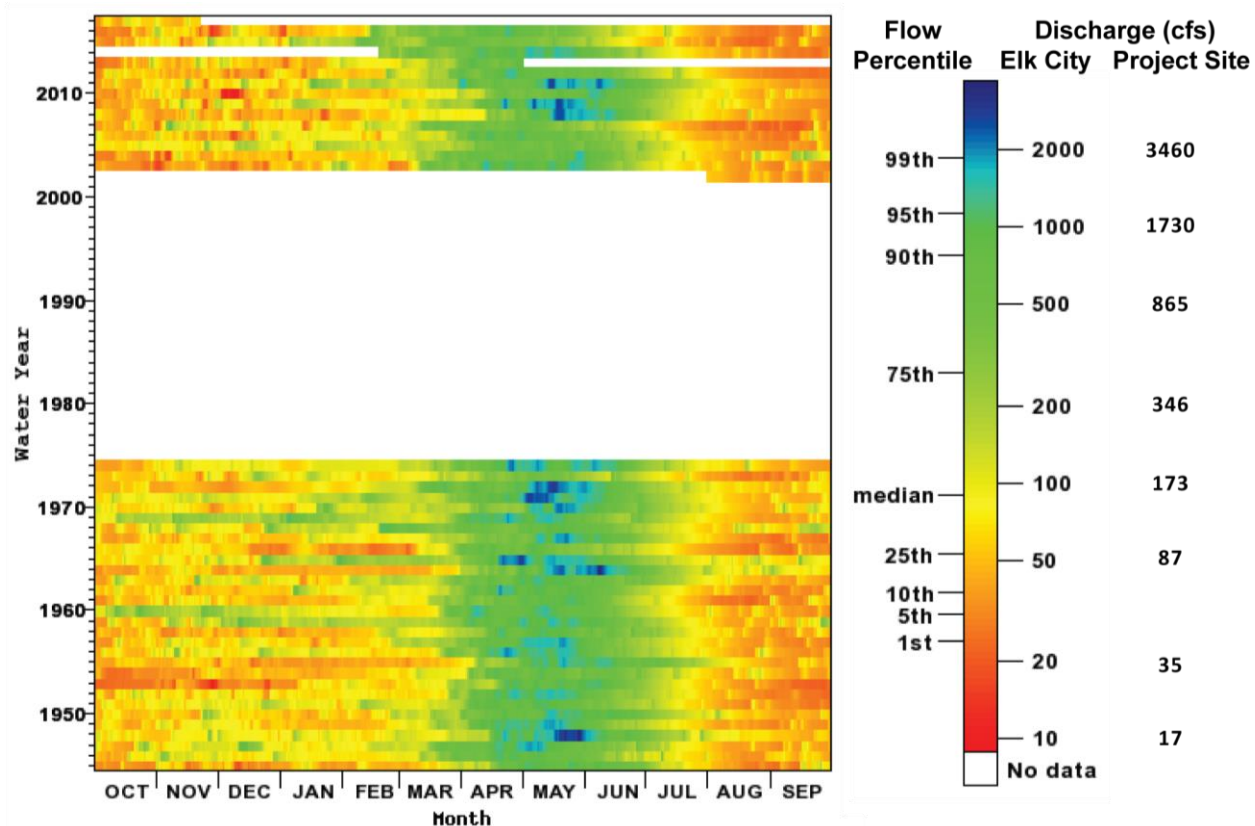


Figure 21. Raster hydrograph showing daily flows (at Elk City, scaled to the project site as indicated) for the period of record. Modified from figure produced by USGS Water Watch (USGS 2016b).

South Fork Clearwater River MP 28 Hypothesized Velocity Barrier

Another way of viewing daily flows at the project site is depicted in Figure 22, which shows daily flow exceedance percentiles for the annual hydrograph.

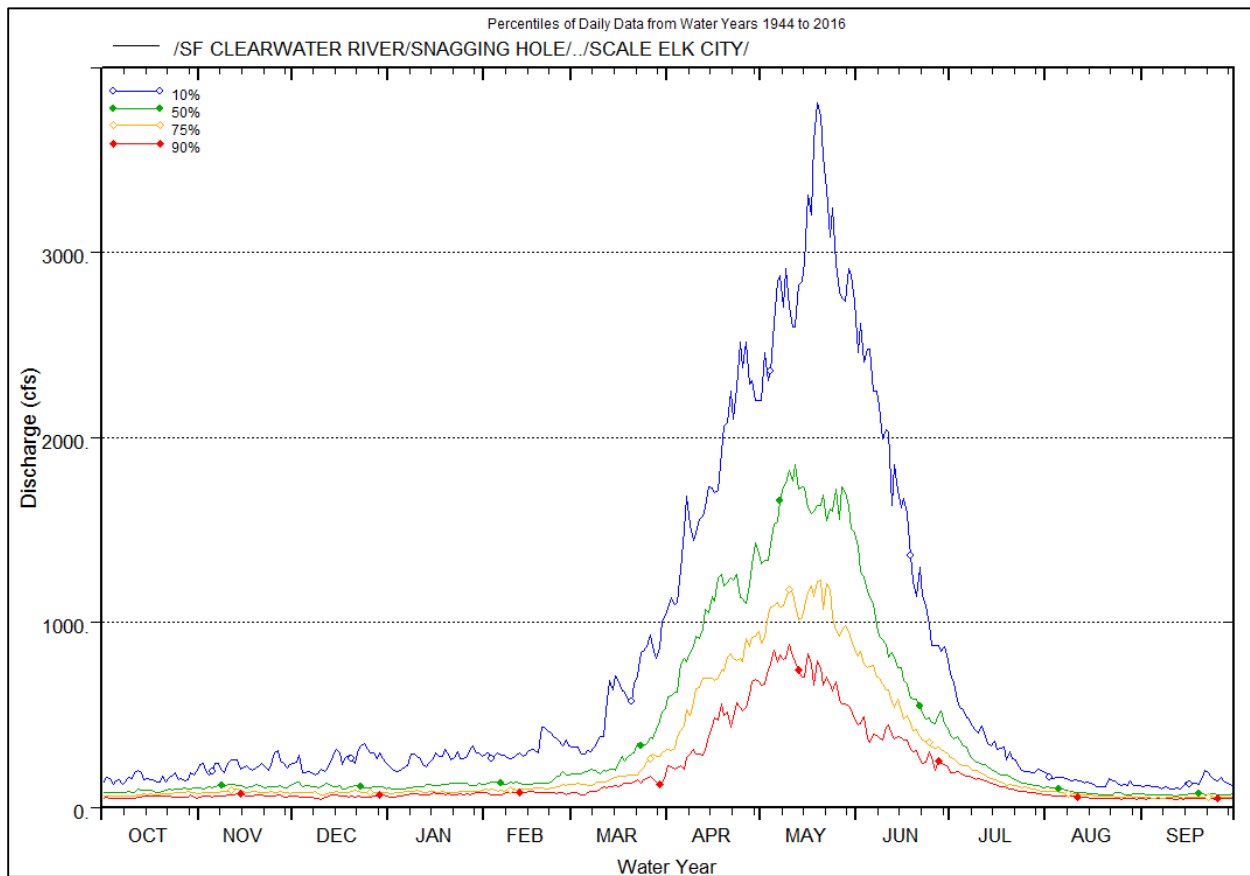


Figure 22. Annual hydrograph at project site with daily percent exceedance curves.

Climate Change Impacts

Figure 23 shows a summary of predicted monthly average flow changes for the three analog sites. These results correspond to a shift of the spring freshet flood peak from May to April by the 2080s – reflecting earlier initiation of snowmelt associated with warming. The ensemble mean daily prediction suggests that the freshet monthly average flow may decrease by 20 to 30 percent by the 2080s. This reflects a future tendency for smaller snowpack accumulation because of a partial shift from snow to rain. Individual predictions range from a slight increase to a 50 percent decrease by the 2080s.

In contrast to the reduction in average freshet flow, the magnitude of large floods (20 to 100 year recurrence interval), is expected to increase (Figure 24), with the most relative change occurring in the biggest floods. Although little change is predicted at Orofino under the A1B emissions scenario, the 20- and 100-year recurrence interval floods are expected to increase by approximately 20 percent and 14 percent, respectively.

 South Fork Clearwater River MP 28 Hypothesized Velocity Barrier

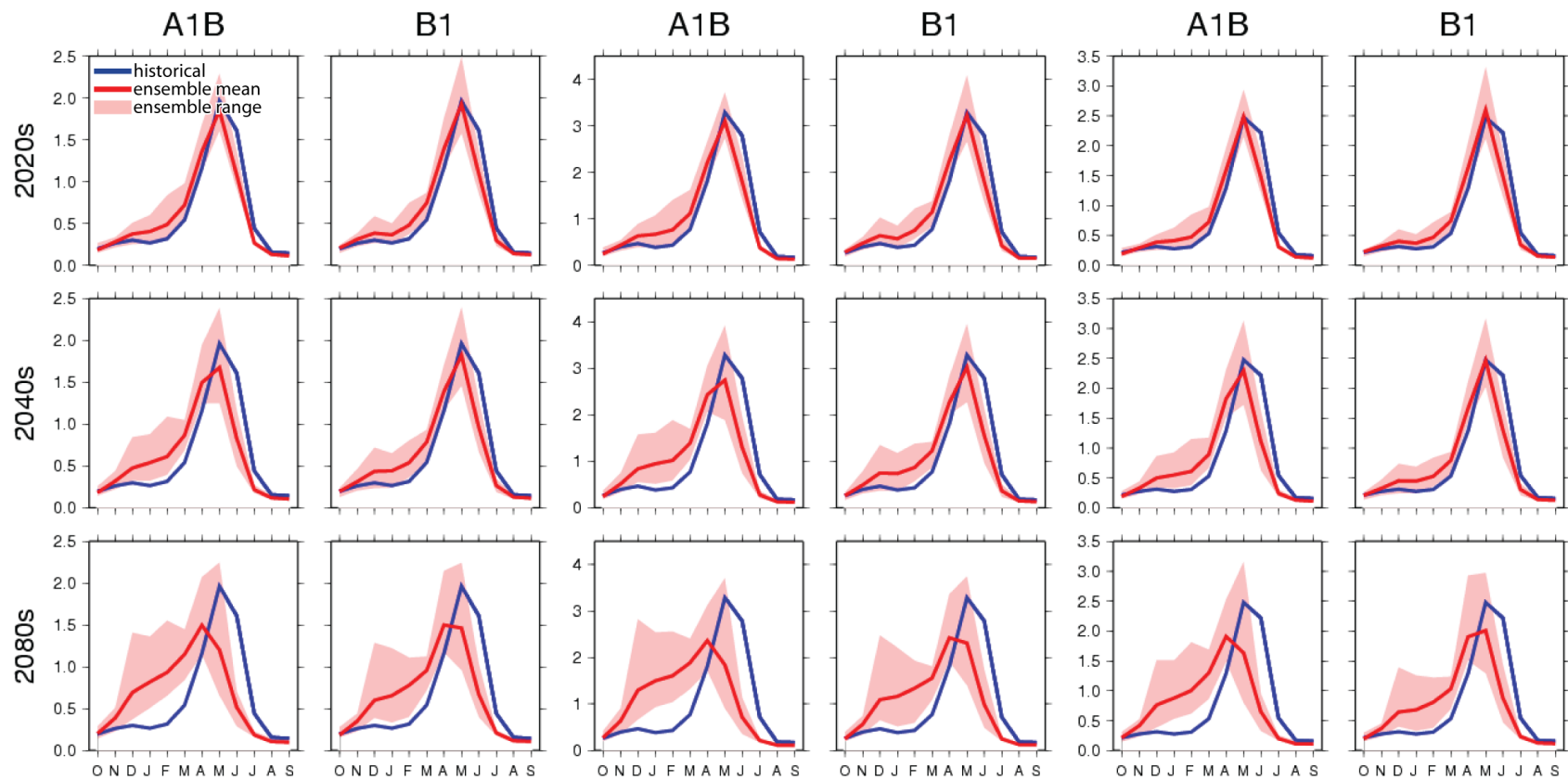


Figure 23. Summary of projected monthly flow (given in inches) changes for the analog watersheds in Table 1. Blue lines show monthly averages for historical conditions, the pink bands show the range of projected change associated with 10 ensemble predictions for each scenario and time period, and red lines show the average of the ensemble predictions. Figure panels downloaded from the Columbia Basin Climate Change Scenarios Project website at <http://warm.atmos.washington.edu/2860/>. These materials were produced by the Climate Impacts Group at the University of Washington in collaboration with the WA State Department of Ecology, Bonneville Power Administration, Northwest Power and Conservation Council, Oregon Water Resources Department, and the B.C. Ministry of the Environment.

 South Fork Clearwater River MP 28 Hypothesized Velocity Barrier

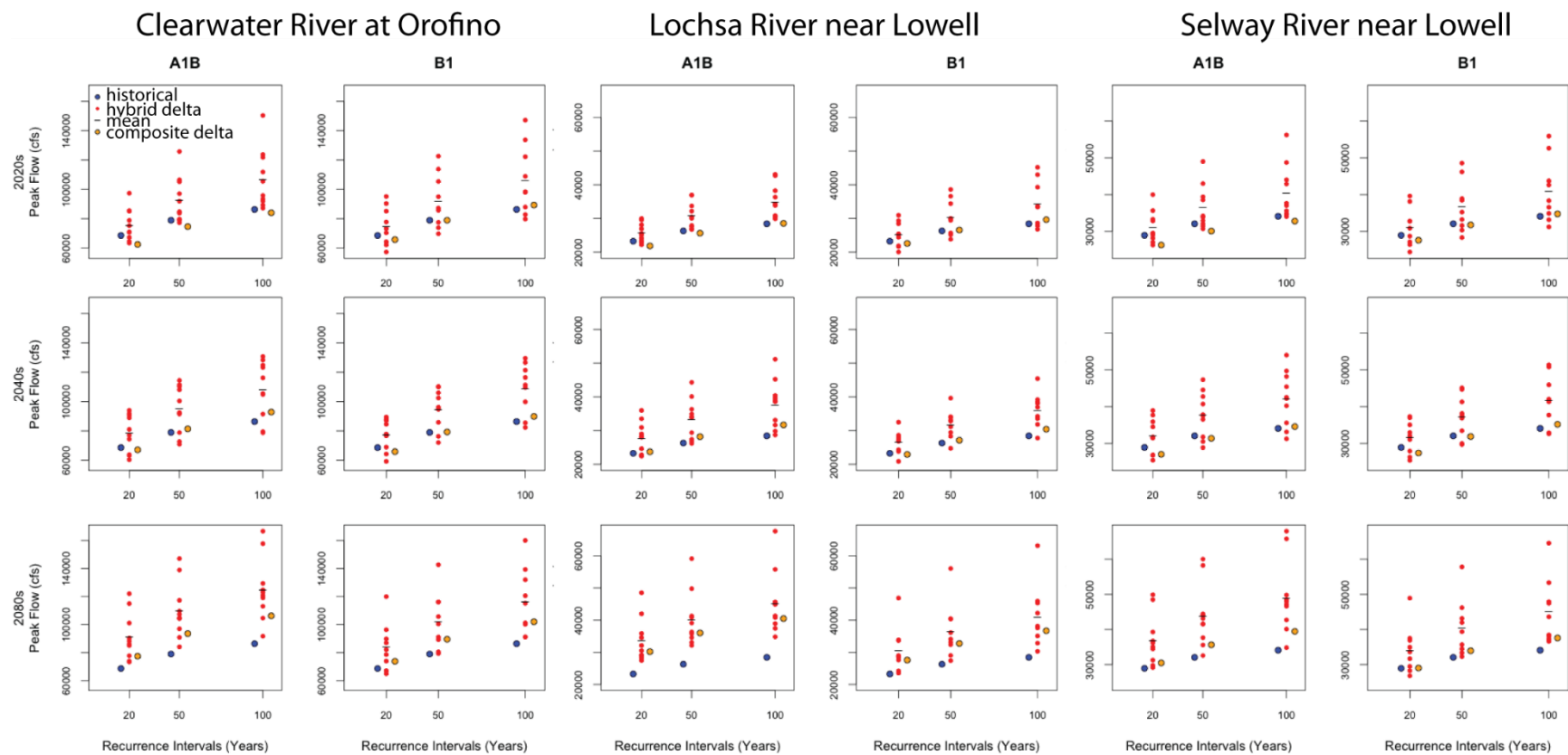


Figure 24. Summary of predicted flood flow changes for several of the analog locations watersheds for the project site. Blue dots represent the historical values, red dots show the range of values from the hybrid delta ensemble predictions, black lines show the mean of the ensemble predictions, and the orange dot shows the single value calculated for the composite delta projections. Figure modified from those panels downloaded from the Columbia Basin Climate Change Scenarios Project website at <http://warm.atmos.washington.edu/2860/>. These materials were produced by the Climate Impacts Group at the University of Washington in collaboration with the WA State Department of Ecology, Bonneville Power Administration, Northwest Power and Conservation Council, Oregon Water Resources Department, and the B.C. Ministry of the Environment.

Hydraulics

Hydraulic conditions were evaluated in the validated hydraulic model by slowly increasing the flow from 74 cfs to 3,190 cfs over the course of 10 simulated hours (59 hours computer computation time). This simulation ends at approximately a 2-year discharge, or the one percent annual exceedance flow. Model simulations were terminated at the 2-year discharge because fish passage is not expected above this. Raster maps of velocity, depth, and water surface elevation were computed at one minute intervals to evaluate development of a fish passage barrier.

Hydraulic model results confirm the presence of a long channel segment with relatively high velocity flow in the reach immediately above Snagging Hole, and of several shorter, but steep high velocity segments between Birdhouse Hole and Snagging Hole. Animations showing change in hydraulic conditions over this range of flows may be accessed from the following links:

Birdhouse Hole to above Snagging Hole Velocity: <https://vimeo.com/195029814>

Velocity color ramping depicts computed in-stream water velocities, in ft/s

Dark blue = 0 ft/s.

Dark red = 19 ft/s

Birdhouse Hole to above Snagging Hole Depth: <https://vimeo.com/195029779>

Depth color ramping depicts computed in-stream water depth, in ft

Light blue = 0 ft.

Dark blue= 12 ft

Birdhouse Hole to above Snagging Hole Water Surface Elevation: <https://vimeo.com/195029859>

Elevation color ramping depicts computed water surface elevation, in ft above sea level

Light green = 3,255 ft above sea level

Dark purple = 3,291 ft above sea level

Below Birdhouse Hole Velocity: <https://vimeo.com/195029825>

(Velocity color ramping same as above.)

Below Birdhouse Hole Depth: <https://vimeo.com/195029790>

(Depth color ramping same as above.)

Below Birdhouse Hole Water Surface: <https://vimeo.com/195029866>

Elevation color ramping depicts computed water surface elevation, in ft above sea level

Light green = 3,232 ft above sea level

Dark purple = 3,259 ft above sea level

Fish Contextualization

Modeling Fish Burst Swimming Performance

In order to begin to answer the question of “*How does channel morphology interact with hydrology to create a velocity barrier or impediment?*” fifteen spatially explicit model outputs (velocity grids) were generated for the study reach at 100 cfs intervals across a range of discharges from 100 cfs to 1500 cfs. Each velocity grid comprised homogeneous patches of modeled velocity derived from the 2-D model thought to impede or block steelhead migration. These results were based on published burst speeds that a 90 cm steelhead could sustain for 5 second, 10 second, and 20 second intervals (Hunter and Mayor 1986). Beginning with the grid representing velocities at 100 cfs, patches of water velocities that exceed the migratory capabilities of steelhead for 20 second durations were evident and increased with discharge. While the number and spatial extent of barrier patches was variable for each velocity grid (see **Error! Reference source not found.**), in general, the frequency (number), spatial extent (size), and visual connectivity of patches increased with discharge (Figure 25, Figure 26).

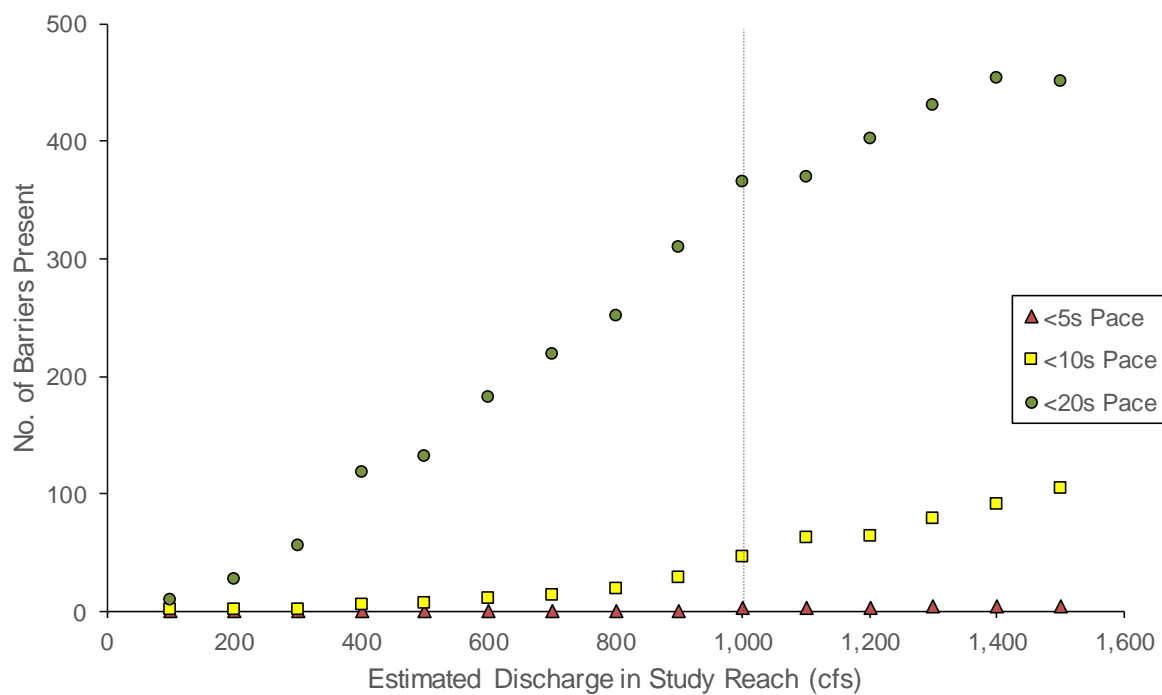


Figure 25. Emergence of barriers within the study reach, based on three of burst swimming paces for a 90 cm steelhead (<5 second pace, <10 second pace, and <20 second pace). Barriers at the 20s and 10s paces represent patches of water with combinations of velocity and length that exceed the swimming capacity of a 90 cm steelhead. Barriers at the 5s pace (maximum burst speed, V_{crit}) represent patches of water with velocity, *per se*, that exceeds the swimming capacity of a 90 cm steelhead. At discharge as low as 100 cfs (within the study reach), ten sufficiently long and fast patches of water emerge to prevent upstream passage of a 90 cm steelhead. At 1,000 cfs, more than 400 barriers are present, including a single patch of water with velocity $>V_{crit}$ (a “*per se* velocity barrier”). By 1,500 cfs, 560 barriers, including four *per se* velocity barrier patches are present within the study reach.

South Fork Clearwater River MP 28 Hypothesized Velocity Barrier

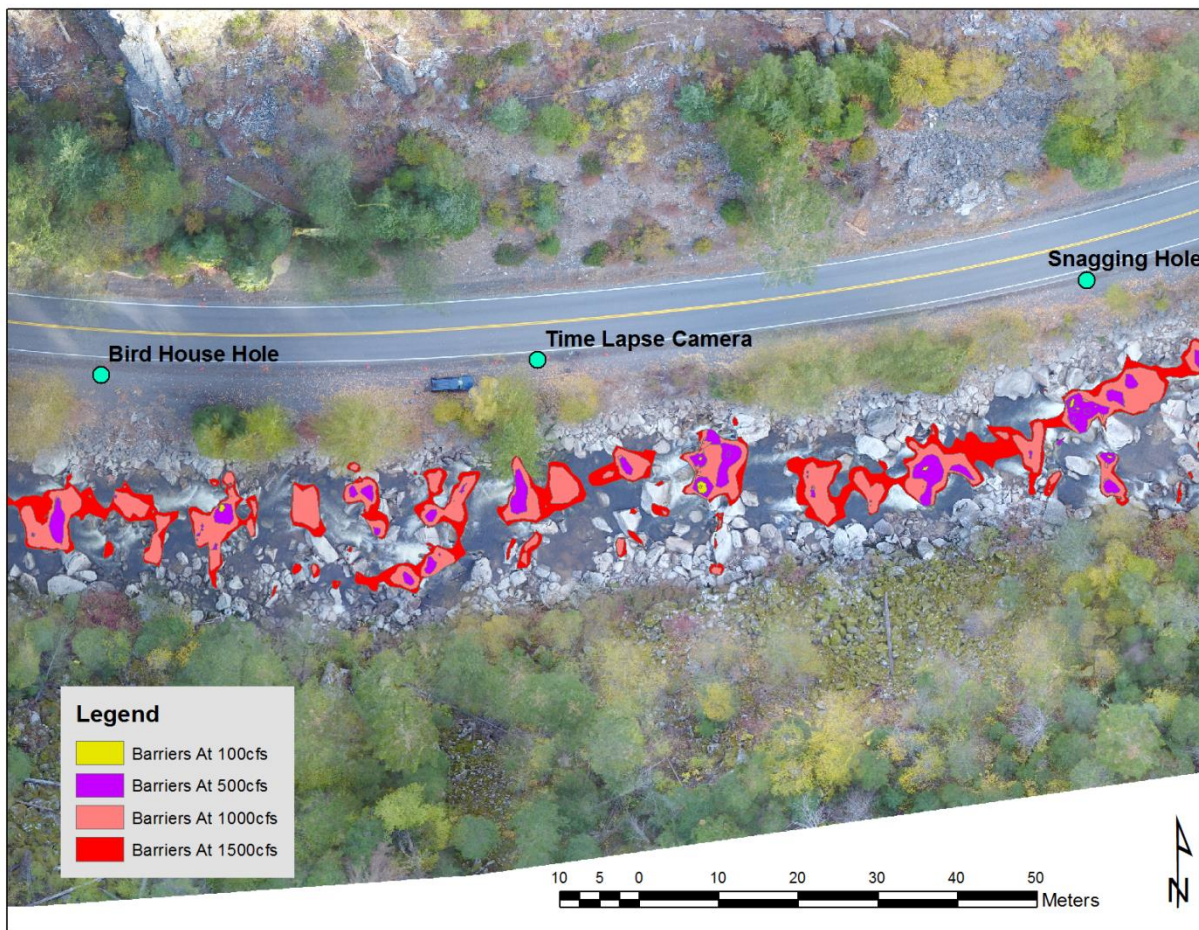


Figure 26. Extents of hydraulic barriers in one area of concern at four different flows ranging from 100 cfs to 1500 cfs. As flows increase, the size and connectivity of hydraulic barriers increases.

Fish Behaviors Inferred from Tracking Data

Fixed radio telemetry antennas tended to record fish detections at a similar rate across each day, with slightly more detections occurring during 20:00 – 22:00 (6% and 5.5% of total detections, respectively; Figure 27).

South Fork Clearwater River MP 28 Hypothesized Velocity Barrier

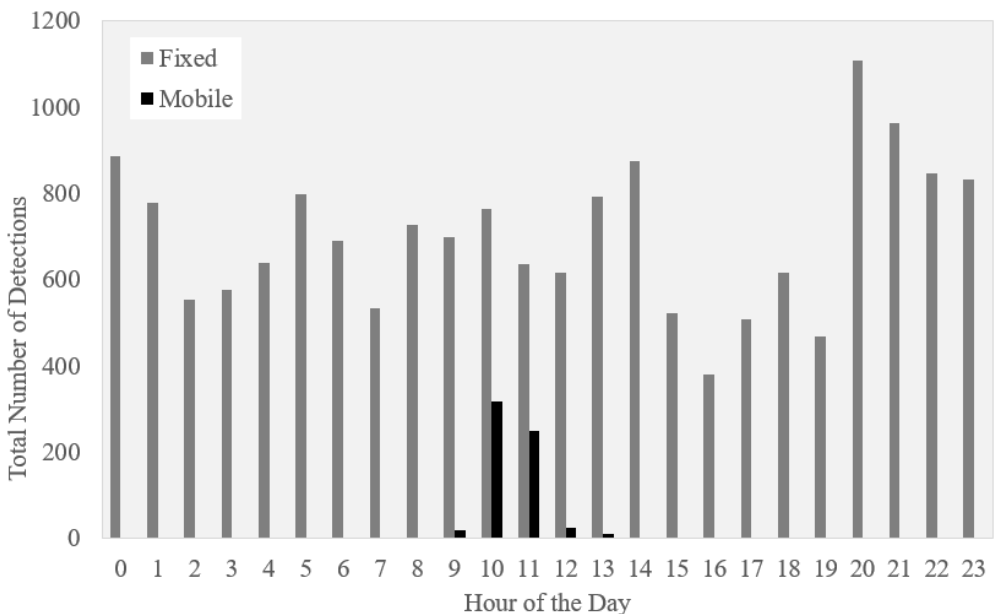


Figure 27. Temporal distribution showing the total number of detections in the study area grouped by fixed and mobile tracking efforts.

Of the 24 fish which entered the study area, 13 (54%) passed the velocity barrier, 6 (25%) entered the study area but were not detected above the barrier, and 5 (21%) remained downstream (Figure 28).

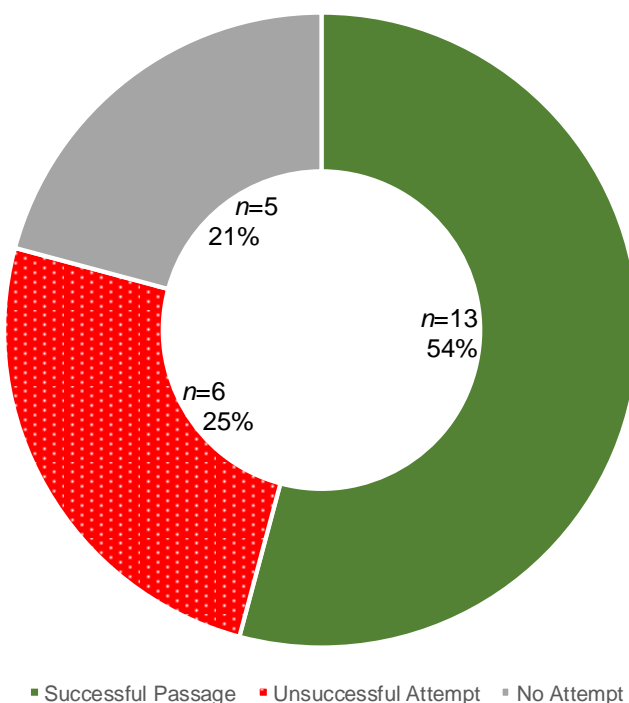


Figure 28. Relative proportion of tagged steelhead that successfully passed the hypothesized barrier (solid green), entered but did not pass (stippled red), and were not detected within the study zone (solid gray).

South Fork Clearwater River MP 28 Hypothesized Velocity Barrier

Regionally relevant discharge in the SF Clearwater River peaked in mid- to late-April 2016, and most fish had entered the study area (irrespective of passage success) by 1 May 2016 (Figure 29). Fish that passed successfully appear to have done so on the descending limb of the hydrograph following small pulses in runoff.

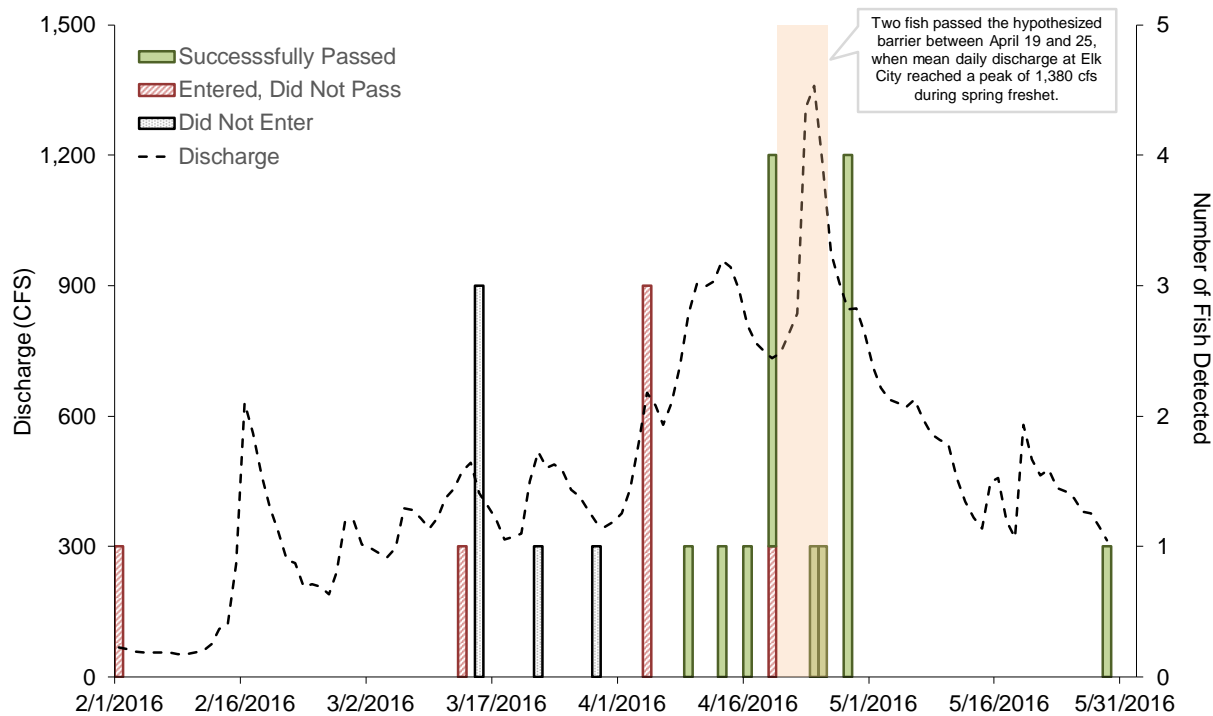


Figure 29. Daily counts of fish detected, grouped by inferred passage category (see legend) and plotted per the right-hand y axis, with daily discharge at Elk City (USGS gage 13337500) plotted per the left-hand y axis. The vertical orange box highlights two fish (#40 and #112) that were first detected upstream of the hypothesized barrier on April 24 and 25 and may have passed during spring freshet, when discharge at Elk City was approximately 1,380 cfs.

South Fork Clearwater River MP 28 Hypothesized Velocity Barrier

Fish detected above the hypothesized barrier appear to have attempted and successfully passed of this zone on dates with relatively high discharge. Mean daily discharge at Elk City when fish may reasonably be inferred to have passed the hypothesized barrier averaged 742 – 837 cfs (Table 4). Two fish (#40 and #112) may have passed when discharge at Elk City was above 1,000 cfs, although it is impossible from the available data to determine actual date of passage. Four of the 13 steelhead detected above the barrier were detected only once, presenting a challenge for inferring the date (and discharge) during passage. Consequently, we analyzed the subset of only those nine steelhead that were detected more than once. Fish that were detected above the barrier and were RT detected more than once were inferred to pass the hypothesized barrier on a date when discharge at Elk City averaged 684 – 820 cfs (Table 4). Moreover, while the two fish described above (#40 and #112) were first detected upstream of the barrier on April 24 and April 25, 2016, when discharge was 1,160 – 1,380 cfs, these fish were last detected downstream of the barrier on April 19, 2016, when discharge was only 733 cfs. Thus, they may have passed when discharge was similar to discharge during inferred passage for other fish. Consequently, we provide an additional summary analysis in Table 4, focusing again on those fish that were detected above the barrier and were RT detected more than once, but omitting fish #40 and fish #112. This group of seven fish were inferred to pass the hypothesized barrier on a date when discharge at Elk City averaged 670 – 692 cfs.

Table 4. RT detections of successfully passing fish immediately prior to, and following the point where fish passed SF Clearwater RKM 71 (RKM 938 from the Pacific Ocean, *i.e.*, the location of the hypothesized velocity barrier), as well as the total number of detections per fish, and mean daily SF Clearwater River discharge on the date of last detection prior to passage and first detection post passage.

Fish#	# Detections	Last Detection		First Detection	
		Date	Downstream of Study Reach Discharge (cfs)	Date	Upstream of Study Reach Discharge (cfs)
26	2	9-Apr	834	9-Apr	834
35	1	28-Apr	845	28-Apr	845
40	1,164	19-Apr	733	25-Apr	1,180
46	1	28-Apr	845	28-Apr	845
62	1	13-Apr	958	13-Apr	958
63	2,589	19-Apr	733	19-Apr	733
95	1	28-Apr	845	28-Apr	845
106	5	28-Apr	845	28-Apr	845
112	23	19-Apr	733	24-Apr	1,360
120	6,384	4-Apr	654	4-Apr	654
121	4	29-May	314	29-May	314
125	4,624	4-Apr	654	9-Apr	834
128	1,439	4-Apr	654	7-Apr	630
Grand Mean (13 Fish)		20-Apr	742	21-Apr	837
Mean for Fish With >1 Detections (9 Fish)		1,804	18-Apr	684	20-Apr
Mean for Fish With >1 Detections, omitting #40 & #112 (7 Fish)		2,150	18-Apr	670	19-Apr
					692

South Fork Clearwater River MP 28 Hypothesized Velocity Barrier

We detected no difference in FL at the time of tagging among fish that successfully passed the hypothesized barrier ($n = 12^3$; mean = 763 mm, $sd = 75$ mm), those inferred to have attempted and failed ($n = 6$; mean = 781 mm, $sd = 44$ mm), and those that were not detected within the study area ($n = 5$; mean = 812 mm, $sd = 48$ mm), using single factor ANOVA ($p = 0.37$; Figure 30).

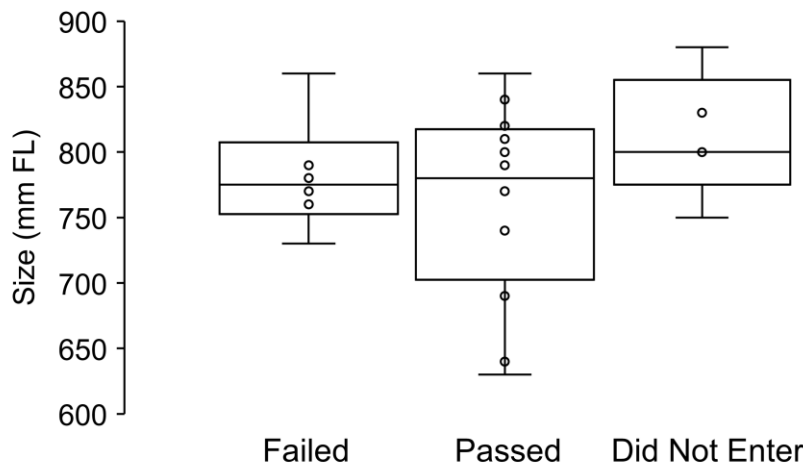


Figure 30. Comparison of fork length (FL) among steelhead that were detected within the study area but not above it (inferred to have attempted and “Failed” passage), steelhead that were detected above the hypothesized barrier (“Passed”), and steelhead not detected in the study area (“Did Not Enter”).

³ FL was missing for one of the 13 fish that were detected above the hypothesized barrier.

South Fork Clearwater River MP 28 Hypothesized Velocity Barrier

Here, we also provide tracking data for an example case, fish #128, which appears to have successfully passed the hypothesized barrier near SF Clearwater RKM 71 (RKM 938 from the Pacific Ocean) in early April 2016, when SF Clearwater River discharge at Elk City was approximately 630 cfs (Figure 31).

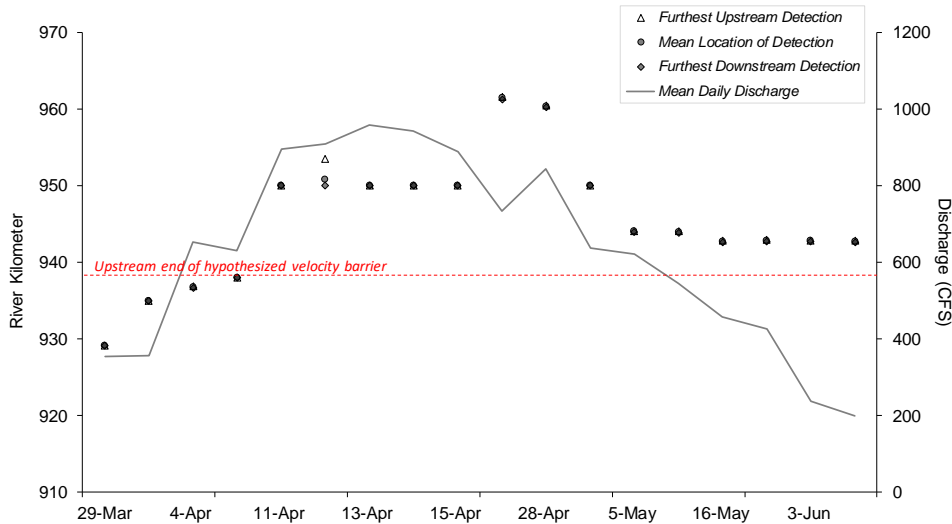


Figure 31. Fish #128's RT detection history, with locations plotted per the left-hand y-axis, and mean daily SF Clearwater River discharge, measured at the Elk City USGS gage (13337500).

DISCUSSION

Is there a barrier? – Does channel morphology near MP 28 interact with regional hydrology to create sufficient velocities that steelhead passage is likely impeded or prevented?

Hydraulic Model Inference

Is there a threshold flow, above which the barrier emerges?

Based on the analysis of computed velocities within the study reach, barriers impeding steelhead passage could emerge at discharge as low as 100 cfs. At discharge within the study reach of 1,000 cfs (similar to flow observed on a near annual basis during spring freshet), a single patch emerges immediately upstream of the “snagging hole,” with water velocity $>V_{crit}$ for a 90 cm steelhead. This patch would represent a barrier to upstream passage for such a fish, solely by virtue of water velocity in the patch. In addition, at 1,000 cfs within the study reach, hundreds of velocity impediments (*i.e.*, patches that may represent barriers by virtue of a combination of water velocity and patch length) are present. Moreover, at these discharges, velocity impediments increasingly begin to merge, and low velocity water suitable for resting and recovering disappear.

Previous studies of upstream fish migration and hydraulic barriers that empirically evaluate natural river channels are extremely rare (but see Reiser et al. 2006) and explicitly evaluate

South Fork Clearwater River MP 28 Hypothesized Velocity Barrier

variables such as a fish's leap angle, plunge pool depth, and horizontal distance to hydraulic crest. Other studies were conducted in laboratories or flumes where hydraulic variables were controlled (e.g., Haro et al. 2004; Weaver 1963). By contrast, our approach implicitly incorporates similar factors affecting hydraulic conditions through the 2-D model and presents them in the predicted velocities across a range of discharges. This is possible due to the extremely high resolution of our datasets that minimize error by explicitly accounting for sources of hydraulic variability caused by the geomorphic features in the channel.

Here, it is important to note five points that inform interpretation of these results:

First, at flows below 1,000 cfs, discharge computed within the study reach corresponds to approximately 2x discharge readings at the Elk City gage (Figure 20). Anecdotal reports from NPT (Mark Johnson, personal communication) indicate that steelhead exhibit diminishingly successful passage at discharge >600 cfs, *as measured at the Elk City gage*. Given the near doubling of flow between Elk City and the study reach, 600 cfs at Elk City is very close to 1,000 cfs within the study reach.

Second, pace matters: In-stream water velocities that exceed the greatest swimming velocity attainable by a 90 cm steelhead are not passable, *per se*. However, velocity barriers may emerge at lower velocities, if sufficient lengths of relatively high velocity water are present. That is, fish burst swimming velocities can be categorized by the temporal duration for which a fish can sustain effort necessary to maintain that velocity. Moreover, even if separated by relatively low velocity water, patches of medium and high velocity water may present either (1) absolute or (2) operational velocity barriers. In the case of the latter, it is important to recognize that fish swimming behaviors do exhibit some degree of volition. If velocities impede passage sufficiently, a fish may "decide" to turn around. Similarly, a fish may be dissuaded from proceeding upstream if it encounters a sufficient string of disconnected high velocity patches.

Third, velocity estimates based on the physical channel model are sensitive to the value of the roughness parameter (**Figure 10**). Importantly, using the data collected during this study, it is possible to assign a range of reasonable values for this parameter. Precise determination of patch level roughness within the study reach requires direct measurements of benthic substrate at a scale beyond that conducted for the present study; in itself, this would be a non-trivial undertaking. This means that, while a high degree of confidence can be imparted to model estimates of *relative* velocity within the reach (*i.e.*, precision of locating fast and slow patches), the *actual* values may be different (*i.e.*, accuracy of quantified velocity estimates). With the model output in hand, it is possible (as shown above) to determine *locations* in the reach where velocity barriers emerge, their approximate *size*, the *sequence* ordering how these patches emerge at increasing flows, and the *manner* in which these patches ultimately stitch together to form a spatially contiguous impediment to steelhead migration. These components can be determined with a high degree of confidence. However, insofar as roughness and discharge interact with channel slope to influence water velocity, estimates of discharge at which barriers emerge should be treated with caution, unless finer resolution of patch-level roughness are obtained. The ultimate enumeration of impassable flow comes from observations of steelhead passing the study reach under various conditions.

Fourth, velocity estimates within the study reach are vertically averaged. In reality, water velocities within the study reach likely exhibit substantial vertical heterogeneity, given the large

clast size of benthic substrate and the high degree of turbulence. Water adjacent to benthic roughness elements is likely close to stationary, although the vertical extent of this boundary layer is unknown, particularly as turbulence increases. The important implication of this is that water near the surface is likely substantially faster than the model predicts. Operationally, what matters for passage is whether a fish can locate and exploit a navigable stratum of sufficiently slow water. In the study reach of the SF Clearwater River, because of its highly constrained channel, at common discharges (*e.g.*, during spring freshet), any navigable slow water may disappear or become unusable. Unfortunately, resolving small scale velocities within the highly turbulent water observed in the study reach remains unknown, and may ultimately be unknowable.

This last statement brings up the fourth and final caveat, which pertains to the complexity of velocities within the study reach, both vertically within the water column and horizontally across the channel. Simple processes can lead to complex outcomes, through small, iterative changes that amplify minute differences in starting conditions, in difficult to predict ways. Deterministic uncertainty (chaos) is a term often used to describe such mechanisms that lead to non-periodic, erratic, and seemingly complex patterns from relatively simple rulesets (Alligood et al. 1997). Chaos-based analytical approaches have been used for a variety of applications (Hirsch et al. 2012), including describing bed load mobilization and transport processes (Gomez and Phillips 1999). Importantly, predictions involving chaotic processes are notoriously difficult (Lorenz 1963a; Lorenz 1963b), and chaotic patterns (Figure 32) tend to emerge in both time and space.

Although chaos math may seem academic, its applications are real and common: Processes and problems as varied as predicting weather and directing missiles rely upon chaos math. Chaos is relevant to the current project, because when a high degree of turbulence is present within a stream, estimating very small scale water velocities within the channel may not only be technically overwhelming, but may operationally be moot. This is because, if truly chaotic, then in-stream water velocities at any time (or location) would tend to exhibit both of the twin hallmarks of chaotic systems, namely nonperiodicity (erraticism) and sensitive dependence upon initial conditions. This means that the velocity at a given location and time depends on the velocity at that location immediately prior, the velocity at all adjacent locations (both upstream and downstream), and on the relationships among these. Complicating matters, in chaotic systems, these states and relationships do not repeat in any periodic fashion. Therefore, a candid acknowledgment of the implications of chaos, and adoption of a semi-quantitative or even qualitative approach for describing in-stream water dynamics and apparent velocities may instead be more appropriately suited for the current type of problem than pursuit of increasingly rigorous and resolved estimates of in-stream water velocities.

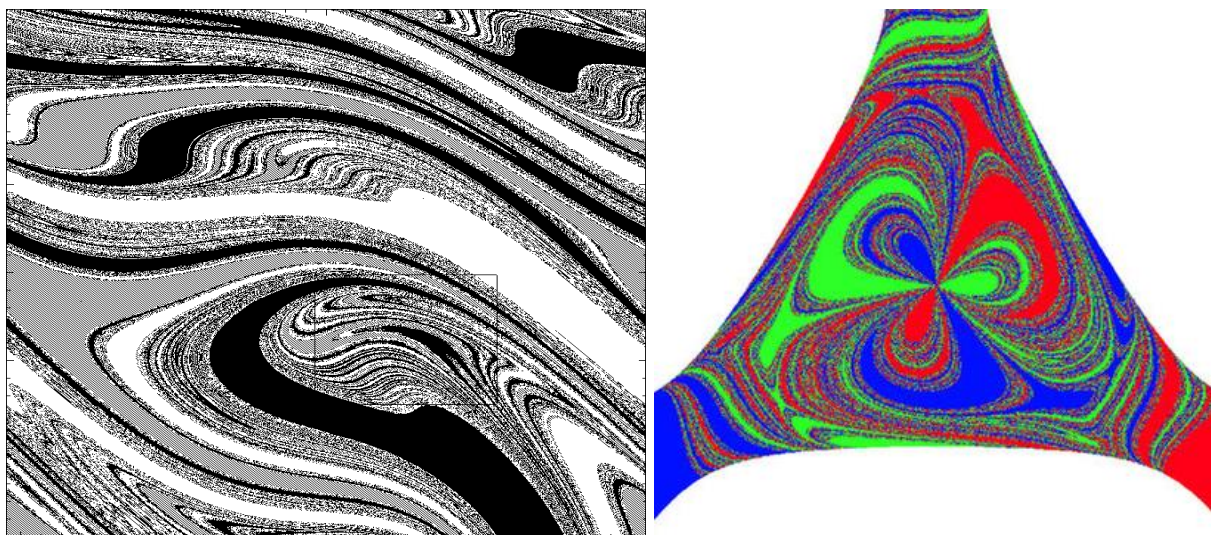


Figure 32. Example of chaotic patterns that can emerge from rulesets involving simple iterations and sensitivity to initial conditions (left panel after Alligood et al. 1997; right panel after Daza et al. 2016).

Tracking Data Inference⁴

Comparison of the frequency of fish entry into the study area and discharge records (see Figure 29) suggest two inferences:

- (1) On the scale of weeks and months, fish tend to enter the study area *during* the peak freshet.
- (2) On the scale of days, fish tend to migrate upstream after a pulse in discharge, *i.e.*, on the descending limb of the hydrograph following a runoff event.

If a velocity barrier exists during the period for which we have tracking data, then one would suspect fish that failed to pass would have encountered greater discharges on their inferred date of attempted passage, compared to discharge on the inferred date of passage for successful fish. Unfortunately, with the available data such an analytical approach would illegitimately rely upon substantial underlying assumptions in order to infer dates of attempted passage among successful and unsuccessful groups, based on relatively sparse tracking data. Specifically, this would require the assumption that the last upstream detection for fish that were not detected above the barrier represents an attempt to pass. Unfortunately, the upstream-most detection of a fish not subsequently detected above the hypothesized barrier does not necessarily equate with the date of an attempt. In reality, these fish may have evaded detection and attempted passage at later dates, when discharge was substantially higher. Thus, it is not possible, with the available data, to definitively determine whether these fish attempted passage, and if so, what discharge was during that attempt.

⁴ Caveats to this analysis: (1) An unknown number of mobile and fixed detections were removed from the dataset by Nez Perce (NP) biologists, as the detections had not been repeated elsewhere. These data were most frequently collected from the first bridge upstream of the velocity barrier site (*i.e.*, Bridge 212). By removing these data points, less fish appear to have passed the barrier. (2) Not all fish that were detected in the study area ($n = 24$) were necessarily attempting to pass the hypothesized barrier as some steelhead spawn on the mainstem. The next nearest tributary downstream is Peasley Creek, ≈ 23 km downstream. There are other tributaries including Meadow Creek and Mill Creek which are further downstream that are known to support spawning. We explicitly note here that sample size is low for these tracking data, and thus power associated with these data are limited.

South Fork Clearwater River MP 28 Hypothesized Velocity Barrier

However, even if comparisons among successful and unsuccessful passage of migrating steelhead are not reliable, meaningful, if anecdotal, insights are still possible from these tracking data, particularly insofar as they enable testing of whether fish can pass at certain discharges. To wit, nine of 13 fish that were detected upstream of the hypothesized barrier were previously detected downstream of the barrier, which enables inference of a range of dates in which those fish may have passed. For six of those nine fish, last detection downstream and first detection upstream were on the same day, meaning that the precise date of passage can be inferred. When focusing on these nine fish, it appears that successful passage through the study area is possible when mean daily discharge at Elk City averages 684 – 820 cfs. Two fish (#40 and #112) may have passed during spring freshet, when discharge at Elk City was 1,380 cfs. However, it is also possible that these fish passed earlier, when discharge was 733 cfs and evaded detection until April 24 or 25. If these fish are omitted from analysis, then mean discharge at Elk City on the inferred date of passage for this group of seven steelhead was 670 – 692 cfs.

Interestingly, our case study fish (#128, see Figure 31) successfully passed the barrier when discharge at Elk City was approximately 630 cfs, then proceeded upstream to approximately SF Clearwater RKM 93 (RKM 960 from the Pacific Ocean) by late April (presumably to spawn, given the duration spent above this headwater detection location), before moving approximately 20 km back downstream by mid-June (possibly kelting).

Do we expect this barrier prevents all fish from passing, or could there be a size threshold?

We detected no difference in FL at the time of tagging between fish that successfully passed the hypothesized barrier and those that did not (Figure 30). Sample size is low ($n = 23$ fish with reported lengths), and thus results are considered provisional or anecdotal. Nonetheless, the available data do not support the hypothesis that the purported velocity barrier may represent an environmental filter that passively selects for large fish.

How frequently, and at what times during the year, does a barrier emerge?

Based on regional hydrology, flows necessary to produce impediment and barrier velocities occur annually. If we consider the 1,000 cfs computed discharge within the reach to represent the flow at which a barrier emerges, this magnitude of flow is expected to occur annually within the study reach during late April/early May with nearly 100% certainty (Figure 22).

Are these also times when we anticipate fish being present in the study area?

The timing of spring freshet (when impediments and barriers emerge) is precisely the time of steelhead spawning migration through the study reach. Tracking data provided by NPT confirm that most fish attempt passage during April, and the run has completed before May 1.

Will the barrier appear more frequently or less frequently in the future?

Climate modeling output suggests regional shifts to earlier and 20-30% smaller spring freshet, concomitant with an increase in the magnitude of moderate to large floods. Because the hydraulic conditions within the barrier area become increasingly difficult for steelhead passage beginning at relatively low discharge in the study reach (see Appendix D), it seems unlikely that such a decrease in the magnitude of peak flows will eliminate hydraulic barriers during steelhead migration. Moreover, if spring freshet occurs earlier, this may lead to an earlier emergence of the barrier, and, given the low discharge threshold associated with its emergence, could lead to longer persistence of the barrier. Of note, alternative climate modeling results for the Clearwater River near Orofino, Idaho predict that by 2050, peak flow intensity will *increase* dramatically, but timing will remain relatively consistent with that exhibited currently (Wu et al. 2012). Since a barrier (or barriers) already sets up on a near annual basis, barring substantial reductions in peak flow intensity, barrier formation will not appreciably diminish. However, under these climate scenarios, it may be possible for the barrier to set up for longer durations, as higher flows occur earlier or with greater frequency.

What do we know about the cause of the barrier?

From available historical records and geographic observations in the reach, it appears that the barrier is the result of valley constriction between the runout of an historic mass wasting event and the road that runs along the right bank valley wall. As exhibited by massive clasts in the channel, this reach frequently receives high energy flows that scour all but the largest boulders.

What can potentially be done about the barrier?

Mitigating for the barriers and impediments within the study area may be possible, *e.g.*, by blasting out large boulders that form the emergent barriers or creating step pool features that enable fish to rest (similar to a fish ladder). However, at least two points are worth considering:

First, is the operationally relevant question of the ability to effectively mitigate, or determining whether action *could* be taken. While there does appear to be a small number of *per se* velocity barriers in the study reach, the underlying channel slope that contributes to high velocities in this reach would remain, as would the more than 500 velocity impediments that emerge at discharges on the order of the annual freshet. While it is hard to imagine that completely eliminating all barriers within the study reach would be a goal of mitigation, given the conclusions derived above that impediments emerge at discharge as low as 100 cfs, it is worth mentioning that complete removal of all barriers does not even seem possible in this reach. Unfortunately, targeting the few *per se* velocity barriers may not result in improved passage, given the high gradient and high concentration of impediments present within the reach.

Second, is the question of whether action *should* be taken. It is unknown to what extent the barrier is anthropogenic. As mentioned above, the evidence does suggest that this reach is constrained in part by construction of the road running along the right bank valley wall. Nonetheless, it remains unclear to what extent relief of that constraint (*e.g.*, if the road were not present) would enable fluvial processes including channel meandering and redistribution of large

boulders greatly enough to alter hydraulics in such a way that would eliminate emergence of high velocity patches of water. If the road is not the cause of these barriers, then this question becomes a values debate, *i.e.*, to what degree *should* managers alter the environment to promote the well-being of a single target species?

What additional studies may be required?

In order to more finely resolve the effects of this reach of very high velocity water on the local population of steelhead, a series of more detailed telemetry studies could be conducted. These could involve capturing fish downstream of the study area (*e.g.*, using a weir), collecting measurements and implanting RT and PIT tags, and then surveying the reach using a combination of additional fixed RT and PIT arrays, applying intense effort to the region bracketing the study reach. In this way, successful and unsuccessful attempts would likely be captured, and precise dates of passage could be inferred. This would accomplish the following:

- (1) Biologically and empirically validate the model, to determine whether fish are operationally blocked from upstream passage by barriers and impediments at predicted locations and discharges.
- (2) Determine precise discharge at which barriers emerge *for these fish*, rather than for the average fish represented in published literature, by comparing discharge on dates of successful and unsuccessful passage.
- (3) Using 1 and 2 above, determine whether mitigation *could* be successfully completed.
- (4) Determine with greater precision whether the barrier acts as a natural selection filter, allowing only large (or particularly high performing) individuals through, which would further help to resolve the question of whether mitigation *should* be done.

In addition, we suggest that, regardless of whether NPT pursues additional tracking studies to determine empirically how, when, and where a barrier emerges within this reach, if NPT decides to pursue mitigation, they should consider adopting a strategic plan for doing so that draws on quantitative assessment and evaluation of alternative scenarios. This could include approaches like heuristic gaming of various mitigation scenarios in order to determine their impacts on instream water velocities. Such an approach could lean substantially on work already completed for this project. By leveraging the model developed for this project and presented in this report, NPT could thereby amass substantial efficiency, while retaining high spatial resolution in a physically validated model. Alternative desktop biological modeling scenarios are also possible, *e.g.*, “urn” simulations that compare performance of randomized groups of individuals drawn from a parent population of fish (with regional size and characteristics) under various modeled channel conditions predicted from alternative mitigation options.

Given the observation that both barriers and impediments cover a non-trivial length of the study reach, in an environment that poses substantial logistical challenges for construction, rigorous evaluation of alternative scenarios and determination of minimum effective effort is recommended.

REFERENCES

- Alligood, K. T., T. D. Sauer, and J. A. Yorke. 1997. Chaos: An Introduction to Dynamical Systems. Springer Berlin Heidelberg, Berlin, Heidelberg.
- Berenbrock, C. 2002. Estimating the Magnitude of Peak Flows at Selected Recurrence Intervals for Streams in Idaho. U.S. Department of the Interior, U.S. Geological Survey. *Prepared in cooperation with:* Idaho Transportation Department, Idaho Bureau of Disaster Services, and U.S. Army Corps of Engineers, Boise, ID.
- Brunner, G. W., and M. J. Fleming. 2010. HEC-SSP Statistical Software Package. US Army Corps of Engineers, Institute for Water Resources, Hydrologic Engineering Center (HEC), Davis, CA.
- Chow, V. T. 1959. Open-Channel Hydraulics. MacGraw-Hill Book Co., Inc., New York, NY.
- Church, M., and A. Zimmermann. 2007. Form and stability of step-pool channels: Research progress. *Water Resources Research* 43(WR005037).
- CIG. 2010. Pacific Northwest (PNW) Hydroclimate Scenarios Project (2860). Climate Impacts Group, College of the Environment, University of Washington, Seattle, WA.
- CRITFC. 2014. Spirit of the Salmon: Wy-Kan-ush-mi Wa-Kish-Wit (2014 Update). Columbia River Inter-Tribal Fish Commission, Portland, OR.
- Daza, A., A. Wagemakers, B. Georgeot, D. Guéry-Odelin, and M. A. F. Sanjuán. 2016. Basin entropy: A new tool to analyze uncertainty in dynamical systems. *Scientific Reports* 6:31416.
- Fonstad, M. A., J. T. Dietrich, B. C. Courville, J. L. Jensen, and P. E. Carbonneau. 2013. Topographic structure from motion: A new development in photogrammetric measurement. *Earth Surface Processes and Landforms* 38(4):421-430.
- Gomez, B., and J. D. Phillips. 1999. Deterministic uncertainty in bed load transport. *Journal of Hydraulic Engineering* 125(3):305-308.
- Haro, A., T. Castro-Santos, J. Noreika, and M. Odeh. 2004. Swimming performance of upstream migrant fishes in open-channel flow: A new approach to predicting passage through velocity barriers. *Canadian Journal of Fisheries and Aquatic Sciences* 61(9):1590-1601.
- Hawkins, E., and R. Sutton. 2011. The potential to narrow uncertainty in projections of regional precipitation change. *Climate Dynamics* 37(1):407-418.
- Hirsch, M. W., S. Smale, and R. L. Devaney. 2012. Differential Equations, Dynamical Systems, and an Introduction to Chaos, Third Edition edition. Academic Press (Elsevier), Waltham, MA.
- Hunter, L. A., and L. Mayor. 1986. Analysis of fish swimming performance data: Volume I. *Prepared by:* North-South Consultants. *Prepared for:* Department of Fisheries and Oceans (Canada) and Alberta Department of Transportation.
- IDFG. 2016. What is an A-run and B-run steelhead? Idaho Fish and Game.
- Jarrett, R. D. 1985. Determination of Roughness Coefficients for Streams in Colorado. *Prepared by:* US Department of the Interior, US Geological Survey. *Prepared in cooperation with:* State of Colorado, Department of Natural Resources, Colorado Water Conservation Board, Lakewood, CO.
- Javernick, L., J. Brasington, and B. Caruso. 2014. Modeling the topography of shallow braided rivers using Structure-from-Motion photogrammetry. *Geomorphology* 213:166-182.
- Kjelstrom, L. C., and R. L. Moffatt. 1981. Method of estimating flood-frequency parameters for streams in Idaho. *Prepared by:* US Department of the Interior, US Geological Survey.

- Prepared in cooperation with:* US Army Corps of Engineers, US Water and Power Resources Service, US Bureau of Land Management, and Idaho Transportation Department, Boise, ID.
- Lorenz, E. N. 1963a. Deterministic nonperiodic flow. *Journal of the Atmospheric Sciences* 20:130-141.
- Lorenz, E. N. 1963b. The predictability of hydrodynamic flow. *Transactions of the New York Academy of Sciences* 25(4 Series II):409-432.
- Morvan, H., D. Knight, N. Wright, X. Tang, and A. Crossley. 2008. The concept of roughness in fluvial hydraulics and its formulation in 1D, 2D and 3D numerical simulation models. *Journal of Hydraulic Research* 46(2):191-208.
- Pix4D. 2016. Pix4Dmapper Pro.
- QSI. 2015. USFS Idaho and Montana Forests LiDAR 2015 (Blocks 2 - 4). Quantum Spatial Company, Inc (QSI), Corvallis, OR.
- Reiser, D. W., C.-M. Huang, S. Beck, M. Gagner, and E. Jeanes. 2006. Defining flow windows for upstream passage of adult anadromous salmonids at cascades and falls. *Transactions of the American Fisheries Society* 135(3):668-679.
- Soto, A. U., and M. Madrid-Aris. 1994. Roughness coefficient in mountain rivers. G. Cotroneo, and R. Rume, editors. *Hydraulic Engineering*, volume Volume 1. American Society of Civil Engineering, New York, NY.
- USACE. 2016. HEC-RAS River Analysis System. US Army Corps of Engineers, Institute for Water Resources, Hydrologic Engineering Center (HEC), Davis, CA.
- USFWS. 2012. Hatchery and Genetic Management Plans (HGMP) for USFWS Lower Snake River Compensation Plan (LSRCP), IDFW -- Upper Salmon River A-run steelhead program, Upper Salmon River B-run steelhead program, and Clearwater River spring Chinook program. US Department of the Interior, US Fish and Wildlife Service, Boise, ID.
- USGS. 1982. Guidelines for Determining Flood Flow Frequency. US Department of the Interior, US Geological Survey, Hydrology Subcommittee.
- USGS. 2016a. USGS 13337500 SF Clearwater River Near Elk City, ID. United States Geological Survey.
- USGS. 2016b. USGS WaterWatch -- Streamflow conditions. United States Geological Survey.
- Weaver, C. R. 1963. Influence of water velocity upon orientation and performance of adult migrating salmonids. *Fishery Bulletin* 63(1):97-121.
- Westoby, M. J., J. Brasington, N. F. Glasser, M. J. Hambrey, and J. M. Reynolds. 2012. ‘Structure-from-Motion’ photogrammetry: A low-cost, effective tool for geoscience applications. *Geomorphology* 179:300-314.
- Wu, H., and coauthors. 2012. Projected climate change impacts on the hydrology and temperature of Pacific Northwest rivers. *Water Resources Research* 48(W11530).

APPENDIX A: PIX4D QUALITY CONTROL REPORT

See: https://www.dropbox.com/s/98trkzx904z8qip/SFM_QC_appendix.pdf?dl=0

(Note: Link Expires January 1, 2018).

APPENDIX B: COMPLETE ORTHOPHOTO MOSAIC

See: <https://share.nhcweb.com/index.php/s/nwv7FnILeDtO9s8>

Password: RunB

(Note: Link Expires January 1, 2018).

APPENDIX C: COMPLETE MERGED SURFACE

See: <https://share.nhcweb.com/index.php/s/nwv7FnILeDtO9s8>

Password: RunB

(Note: Link Expires January 1, 2018).

APPENDIX D: FREQUENCY OF VELOCITY BARRIERS AT INCREASING DISCHARGE

Table 5. Summary table, depicting the emergence at increasing discharge of discrete patches within the study reach that could impede upstream swimming at three burst swimming paces.

Discharge	Burst Swimming Pace	Number of Barriers Present
100	<5s Pace	0
	<10s Pace	1
	<20s Pace	9
200	<5s Pace	0
	<10s Pace	1
	<20s Pace	27
300	<5s Pace	0
	<10s Pace	1
	<20s Pace	56
400	<5s Pace	0
	<10s Pace	5
	<20s Pace	118
500	<5s Pace	0
	<10s Pace	6
	<20s Pace	131
600	<5s Pace	0
	<10s Pace	11
	<20s Pace	182
700	<5s Pace	0
	<10s Pace	14
	<20s Pace	218
800	<5s Pace	0
	<10s Pace	19
	<20s Pace	251
900	<5s Pace	0
	<10s Pace	28
	<20s Pace	309
1000	<5s Pace	2
	<10s Pace	46
	<20s Pace	365
1100	<5s Pace	2
	<10s Pace	62
	<20s Pace	369
1200	<5s Pace	3
	<10s Pace	64
	<20s Pace	402
1300	<5s Pace	4
	<10s Pace	78
	<20s Pace	430
1400	<5s Pace	4
	<10s Pace	91
	<20s Pace	453
1500	<5s Pace	4
	<10s Pace	105
	<20s Pace	451